NeuroImage: Clinical 9 (2015) 436–449

Contents lists available at ScienceDirect

NeuroImage: Clinical

journal homepage: www.elsevier.com/locate/ynicl

Predictive timing functions of cortical beta oscillations are impaired in Parkinson's disease and influenced by L-DOPA and deep brain stimulation of the subthalamic nucleus

Impaired beta-band timing functions in PD

A. Gulberti[a,*], C.K.E. Moll[a], W. Hamel[b], C. Buhmann[c], J.A. Koeppen[b], K. Boelmans[c,d], S. Zittel[c,e], C. Gerloff[c], M. Westphal[b], T.R. Schneider[a], A.K. Engel[a]

[a]Department of Neurophysiology and Pathophysiology, University Medical Center Hamburg-Eppendorf, Martinistr. 52, Hamburg 20246, Germany
[b]Department of Neurosurgery, University Medical Center Hamburg-Eppendorf, Martinistr. 52, Hamburg 20246, Germany
[c]Department of Neurology, University Medical Center Hamburg-Eppendorf, Martinistr. 52, Hamburg 20246, Germany
[d]Department of Neurology, University Hospital of Würzburg, Josef-Schneider-Strasse 11, Würzburg 97080, Germany
[e]Department of Paediatric and Adult Movement Disorders and Neuropsychiatry, Institute of Neurogenetics, University of Lübeck, Maria-Goeppert-Strasse 1, 23562 Lübeck, Germany

ARTICLE INFO

Article history:
Received 23 March 2015
Received in revised form 11 September 2015
Accepted 15 September 2015
Available online 25 September 2015

Keywords:
Parkinson's disease
Interval timing
Beta oscillations
Subthalamic nucleus
Deep brain stimulation

ABSTRACT

Cortex-basal ganglia circuits participate in motor timing and temporal perception, and are important for the dynamic configuration of sensorimotor networks in response to exogenous demands. In Parkinson's disease (PD) patients, rhythmic auditory stimulation (RAS) induces motor performance benefits. Hitherto, little is known concerning contributions of the basal ganglia to sensory facilitation and cortical responses to RAS in PD. Therefore, we conducted an EEG study in 12 PD patients before and after surgery for subthalamic nucleus deep brain stimulation (STN-DBS) and in 12 age-matched controls. Here we investigated the effects of levodopa and STN-DBS on resting-state EEG and on the cortical-response profile to slow and fast RAS in a passive-listening paradigm focusing on beta-band oscillations, which are important for auditory–motor coupling. The beta-modulation profile to RAS in healthy participants was characterized by local peaks preceding and following auditory stimuli. In PD patients RAS failed to induce pre-stimulus beta increases. The absence of pre-stimulus beta-band modulation may contribute to impaired rhythm perception in PD. Moreover, post-stimulus beta-band responses were highly abnormal during fast RAS in PD patients. Treatment with levodopa and STN-DBS reinstated a post-stimulus beta-modulation profile similar to controls, while STN-DBS reduced beta-band power in the resting-state. The treatment-sensitivity of beta oscillations suggests that STN-DBS may specifically improve timekeeping functions of cortical beta oscillations during fast auditory pacing.

1. Introduction

Akinesia, the inability to initiate and execute movements, is a key aspect of impaired motor performance in patients suffering from Parkinson's disease (PD). Once set in motion, kinetic function in PD is abnormally slow and reduced in amplitude. Furthermore, dynamic motor output of PD patients shows a disturbed temporal coordination, resulting in a set of characteristic movement irregularities (Sacks, 1999). Gait and speech of PD patients are often hastened, rapid alternating movements are difficult to perform, and motor synchronization to sensory stimuli is globally impaired. A candidate neuronal mechanism involved in these dysregulations of motor rhythmicity in PD patients may encompass pathological levels of oscillatory brain activity within coupled subcortical and cortical networks (Brown, 2003; Nagasaki et al., 1978).

A characteristic signature of ongoing neuronal activity in the dopamine-depleted motor circuitries of PD patients is abnormal coupling at beta frequencies (13–30 Hz). Beta activity is excessively synchronized within and between functionally interconnected nodes in the basal ganglia (BG), thalamus and cortex, eventually resulting in impaired motor function (Hutchison et al., 2004; Kühn et al., 2006; Little et al., 2012; Sharott et al., 2014). Both dopaminergic medication and deep brain stimulation of the subthalamic nucleus (STN-DBS) reduce beta-band coupling within and between structures of this functional loop in PD patients. At the same time, these neuromodulatory

* Corresponding author at: Department of Neurophysiology and Pathophysiology, University Medical Center Hamburg-Eppendorf, Martinistr. 52, Hamburg 20246, Germany. Tel.: +49 40 7410 55622; fax: +49 40 7410 57752.
E-mail address: a.gulberti@uke.de (A. Gulberti).

http://dx.doi.org/10.1016/j.nicl.2015.09.013

interventions restore physiological motor output, supporting the functional significance of beta oscillations for information processing in the motor domain (Engel and Fries, 2010; Jenkinson and Brown, 2011). Beyond the antikinetic effects of elevated beta-band activity in the resting brain state, their dynamic modulation is impaired in PD as well (Doyle et al., 2005). Impaired beta modulation may lead to deficient dynamic scaling and sequencing of complex sensorimotor processes such as gait (Singh et al., 2013), speech (Hebb et al., 2012) and repetitive movements (Joundi et al., 2013).

External sensory stimuli can temporarily ameliorate some of the motor disabilities of PD patients (Cunnington et al., 1995; Martin, 1967). As an example, rhythmic auditory stimulation (RAS) improves dysrhythmic locomotion and is frequently used to treat gait disturbances in advanced stages of PD (McIntosh et al., 1997). However, sensory facilitation by RAS depends on the stimulation frequency — with slower presentation rates being more effective than fast rhythms (Enzensberger and Fischer, 1996). Hitherto, little is known concerning the neural processing of RAS in PD patients. More specifically, BG-cortex circuits play a critical role modulating beta-band activity during synchronization tasks as timekeeper for movements (Bartolo et al., 2014; Rao et al., 1997; Teki, 2014), but it remains unknown how STN-DBS and dopaminergic medication influence the cortical response profile to RAS in the absence of overt movement.

As a first step, we re-addressed the question whether treatment with levodopa or STN-DBS induces significant changes in ongoing EEG activity focusing, in particular, on the beta-band. To this end, we analyzed the resting state EEG of patients with advanced PD before (DOPA-OFF versus DOPA-ON) and after STN-DBS surgery (OFF-DBS versus ON-DBS). In order to examine the specific influence of BG circuit modulation on rhythm-related auditory processing, we then explored the neurophysiological signatures of RAS in a passive listening paradigm with slow (≤2 Hz) and fast (≥4 Hz) stimulus presentation rates under these four experimental conditions. Since beta-oscillatory signals reflect timekeeping functions in healthy people (Fujioka et al., 2012), we hypothesized that RAS would reveal an altered beta-band response profile in patients with PD.

2. Material and methods

All statistical values are given as mean ± SD unless noted otherwise. Auditory evoked potential analysis of this dataset has been reported elsewhere (Gulberti et al., 2015).

2.1. Patients & control participants

The present investigation was conducted in agreement with the Code of Ethics of the World Medical Association (Declaration of Helsinki, 1967) and the local ethics committee approved the procedures. All participants provided written informed consent. Twelve patients (7 female, 5 male, mean age: 61 ± 6 years) with a diagnosis of advanced idiopathic PD (mean disease duration: 14 ± 3 years, Hoehn & Yahr stage: 3 ± 1; Hoehn and Yahr, 1967) and twelve healthy control persons matched in sex, age and education (8 female, 4 male, mean age: 65 ± 8 years) participated. All participants declared normal hearing and normal or corrected-to-normal vision. Patients underwent bilateral microelectrode-guided implantation of DBS electrodes in the STN. Pre-operatively, all PD patients showed a significant improvement of the motor-subscore (III) of the Unified Parkinson's Disease Rating Scale (Fahn et al., 1987) following intake of levodopa. The mean motor score after overnight withdrawal of anti-parkinsonian medication was 32 ± 12, while after intake of levodopa it was reduced to 18 ± 9 ($t(11) = -5.54$; $p = 0.0002$; paired t-test). This was a mean symptom improvement of 44%. Pre-operatively, the daily levodopa-equivalent dose was 1132 ± 420 mg. During the period of post-operative recordings, it was reduced to 663 ± 354 mg ($t(22) = 2.96$; $p = 0.0073$; paired t-test; conversion factors used for the calculation of levodopa equivalent daily dose after Tomlinson et al., 2010). Importantly, all patients demonstrated an adequate global intellectual capacity, when tested with the Mini-Mental Status Exam (Folstein et al., 1975; mean score: 29 ± 1) and the Mattis Dementia Rating Scale (Mattis, 1988; mean score: 143 ± 0.5). Furthermore, they fulfilled other inclusion criteria for STN-DBS, such as no structural alterations on magnetic resonance imaging (MRI), and no concomitant severe medical comorbidities. Further clinical details are summarized in Table 1.

2.2. Surgical procedures

For all patients DBS electrodes (model 3389, Medtronic, Minneapolis, MN, USA) and stimulators (Kinetra model 7428 in 7 patients and Activa PC model 37,601 in 5 patients, Medtronic, Minneapolis, MN, USA) were implanted at the Department of Neurosurgery at the University Medical Center Hamburg-Eppendorf, Germany. In short, an MRI-compatible Zamorano–Dujovny frame (Stryker Leibinger) was tightly secured with pins on the patient's head. Gadolinium-enhanced volumetric T1 MRI and T2-weighted spin echo MRI sequences were first acquired, and were then fused with computerized tomography scans by means of iPlan (Brainlab), a commercial treatment planning software. Through this procedure, both commissures, the STN-nigra complex and blood vessels could be delineated with high resolution. A reference line connecting the anterior and posterior commissure (AC–PC line) was then determined. The intended target coordinates for the STN were 11.5–12.5 mm from the midline, 1–2 mm behind the midcommissural point and 2 mm below the line connecting anterior and posterior commissure. For the surgical implantation of the electrodes, burr holes of 8–10 mm diameter were fashioned 1–3 cm anterior to the left and right coronal suture. Further details concerning the surgical procedure are reported in Hamel et al. (2003).

Successful placement of the implanted DBS electrodes in the region of the STN was assessed by intra-operative microelectrode recordings, by effective intra-operative macrostimulation, by stereotactic reconstruction of electrode contacts on post-operative stereotactic CT scans fused with pre-operative MRIs, and by a significant improvement in the post-operative UPDRS motor score in DOPA-OFF condition: ON-DBS (20 ± 8) vs. OFF-DBS (40 ± 10; $t(9) = -7.89$; $p < 0.0001$; paired t-test). Two patients were excluded from this paired t-test due to missing post-operative UPDRS scores. Post-operatively, none of the patients showed signs of accidental stimulation of fiber tracks running in the neighboring internal capsule or lemniscal radiation.

2.3. Protocol

The first experimental sessions took place 6 ± 5 days before the implantation of bilateral STN-DBS electrodes for treatment of PD, the second experimental sessions 5 ± 2 months following DBS surgery. In the pre-operative recording sessions, patients were assessed in (i) DOPA-ON and (ii) DOPA-OFF conditions. These two pre-operative recordings always took place on two subsequent days and the order in which the two conditions were recorded was counterbalanced. PD patients were tested after an overnight period of withdrawal from medication (DOPA-OFF condition). It is of note that all post-operative recordings also took place after overnight withdrawal of anti-parkinsonian medication on two different days. Post-operatively, the two experimental conditions were: (iii) ON-DBS, i.e., during bilateral therapeutic STN-DBS with high-frequencies (130–240 Hz) and (iv) OFF-DBS, i.e., with the DBS device switched off. For each subject, stimulation contacts, amplitude and pulse duration were the same as for therapeutic high-frequency stimulation (see Table 1). After switching off the therapeutic high-frequencies DBS, a period of time ≥25 min was elapsed before starting the recordings in the OFF-DBS condition. This period has previously been demonstrated to be long enough to induce a significant worsening of motor symptoms following

Table 1
Clinical and demographic characteristics.

Case	Gender age	Disease duration (years)	H&Y	Pre-op medication (LEDD)	Pre-op UPDRS		DBS parameters for: left electrode (first row); right electrode (second row)	Post-op medication (LEDD)	Post-op UPDRS		
					Dopa-OFF	Dopa-ON			Dopa-OFF OFF-DBS	Dopa-OFF ON-DBS	Dopa-ON ON-DBS
1	m, 66	11	3.5	2022 mg	28	14	130 Hz, 1−, 4.0 V, 60 μs 130 Hz, 5−, 2.8 V, 60 μs	1357 mg	28	13	N/A
2	m, 60	12	2	1049 mg	26	9	240 Hz, 1+, 2−, 3−, 4.9 V, 120 μs 240 Hz, 5+, 6−, 7−, 4.4 V, 120 μs	962 mg	N/A	N/A	N/A
3	f, 57	12	2.5	1422 mg	20	9	130 Hz, 1−, 2−, 2.2 V, 60 μs 130 Hz, 5−, 6−, 2.2 V, 60 μs	582 mg	N/A	2	1
4	f, 54	20	3	1241 mg	22	11	130 Hz, 1−, 2−, 3.0 V, 60 μs 130 Hz, 5−, 6−, 2.6 V, 60 μs	597 mg	26	23	17
5	f, 66	14	3	760 mg	48	27	130 Hz, 1−, 2−, 3.9 V, 60 μs 130 Hz, 6−, 7−, 3.6 V, 90 μs	938 mg	44	25	19
6	f, 69	12	3	806 mg	47	42	200 Hz, 1−, 2−, 3.2 V, 60 μs 200 Hz, 5−, 6−, 3.0 V, 60 μs	660 mg	38	24	16
7	m, 68	6	2	972 mg	32	18	210 Hz, 1−, 2−, 3.2 V, 60 μs 210 Hz, 5−, 6−, 3.2 V, 60 μs	549 mg	33	12	10
8	m, 56	20	3	1131 mg	57	17	130 Hz, 1−, 3.2 V, 60 μs 130 Hz, 9−, 3.5 V, 60 μs	635 mg	57	25	10
9	f, 68	13	4	1431 mg	26	16	130 Hz, 2−, 1.9 V, 60 μs 130 Hz, 10−, 1.9 V, 60 μs	497 mg	44	27	19
10	m, 57	15	3	1437 mg	23	18	130 Hz, 1−, 2−, 3.0V, 60 μs 130 Hz, 9−, 10−, 3.0V, 60 μs	943 mg	52	32	27
11	f, 59	11	3	397 mg	26	12	200 Hz, 2−, 2.0 V, 60 μs 200 Hz, 10−, 2.5 V, 60 μs	56 mg	41	22	15
12	f, 53	11	2	912 mg	31	17	130 Hz, 1−, 2−, 2.3 V, 60 μs 130 Hz, 9−, 10−, 2.5 V, 60 μs	180 mg	37	18	14

Column "H&Y": Hoehn & Yahr stages. Columns "Pre-op medication", "Post-op medication": levodopa equivalent daily doses (LEDD). Column " DBS parameters": stimulation frequency (Hz), active contacts, impulse amplitude (V), impulse width (μs) for left and right electrode, respectively. For the left electrode (first row), contact 0 was the most ventral and contact 3 was the most dorsal. For the right electrode (second row), contact 4 (or 8 in case of Activa PC stimulator) was the most ventral and contact 7 (or 11 in case of Activa PC stimulator) was the most dorsal.

discontinuation of STN-DBS (Temperli et al., 2003), and this is also in line with clinical observations in our patient group.

2.4. Experimental setup and stimuli

The EEG-recordings took place in a darkened, sound-attenuated chamber. Participants were comfortably seated in front of a 21-inch monitor at a viewing distance of 155 cm, and written instructions of the task were presented. Participants were asked to fixate at a white cross (diameter: 3 cm) and to listen passively to the presented auditory stimuli without moving. Stimuli consisted of rhythmic metronome-like clicks presented at 11 different stimulation rates, from 1 to 6 Hz rhythms in steps of 0.5 Hz. For each rhythm-block, a series of 75 clicks were presented. The order of the blocks was pseudo-randomized across sessions and participants. Blocks were separated by a silent pause of 6 s. Single clicks with a duration of 13 ms each, were presented at 70 dB (SPL) through two loudspeakers located in front of the participant's head (Bose companion 2, series II, Framingham, MA, USA). At the end of the task, participants were asked to sit quietly and fixate the white cross in front of them for 1 min in order to record ongoing EEG. Tri-axial accelerometers fixed on both index fingers (Freescale Semiconductor, MMA7260QT) permitted both on-line monitoring and post-hoc quantitation of resting tremor episodes during the recordings. Participants' awareness was constantly tracked throughout the experimental session with the help of EEG and electrooculogram (EOG) parameters and video/intercom surveillance.

2.5. EEG recordings

EEG activity was recorded referenced to the nose tip from 62 active Ag/AgCl scalp electrodes mounted in an elastic cap with equidistant montage (EASYCAP GmbH, Herrsching, Germany). The electrodes had integrated impedance converters fitted directly into the electrode in order to minimize noise from the surrounding area as well as from movement artifacts. This aspect was of particular importance for EEG recordings in PD patients with resting tremor (see below). In order to record EOG activities, two electrodes were placed below the eyes. Accelerometer signals were collected simultaneously with the EEG activity. The data were bandpass-filtered (0.016–250 Hz) and digitized (sampling rate: 1000 Hz) using BrainAmp amplifiers (BrainProducts, Munich, Germany). Signal analyses were performed using Matlab 7.10 (MathWorks, Natick, MA), and two freely available open source toolboxes, EEGLAB 6.03b (Delorme and Makeig, 2004) and FieldTrip (Oostenveld et al., 2011). Statistical analysis of the EEG was restricted to a central region of interest (ROI), comprising the electrodes with the largest auditory responses. This ROI included the averaged signal of the vertex electrode Cz and of six neighboring electrodes (see Fig. 1A). The sensor-level analysis of EEG data in our study precludes precise statements concerning the specific neural sources. However, it is likely that neuronal activity from frontal cortical areas, supplementary motor area and perhaps more posteriorly located motor areas was picked up by sensors within the central ROI. Thus, the chosen ROI was strategically positioned to sample activity from cortical areas and neural systems with particular relevance to interval timing, rhythm perception, and auditory–motor coordination (Fujioka et al., 2012; Grahn and Brett, 2007; Harrington et al., 1998; Rao et al., 1997; Schaal et al., 2004; Toma et al., 2002).

2.6. Artifact removal

A two-step procedure was performed to remove artifacts (Schneider et al., 2008). First, epochs containing non-stereotyped artifacts (e.g., cable movement, swallowing) were removed. Compromised electrode traces were replaced by interpolated data. After the reduction of the number of components to 32 by principal component analysis, extended infomax independent component analysis (ICA) was applied using a weight change $<10^{-6}$ as stop criterion. Independent components representing artifacts (e.g., DBS artifacts, eye blinks, saccadic activity, ECG artifacts) were removed from the EEG data by back projecting all but these components. Low-pass filtering (cut-off frequencies at 100 and 48 Hz for time–frequency and power spectrum analysis, respectively) strongly reduced DBS-related artifacts. Despite

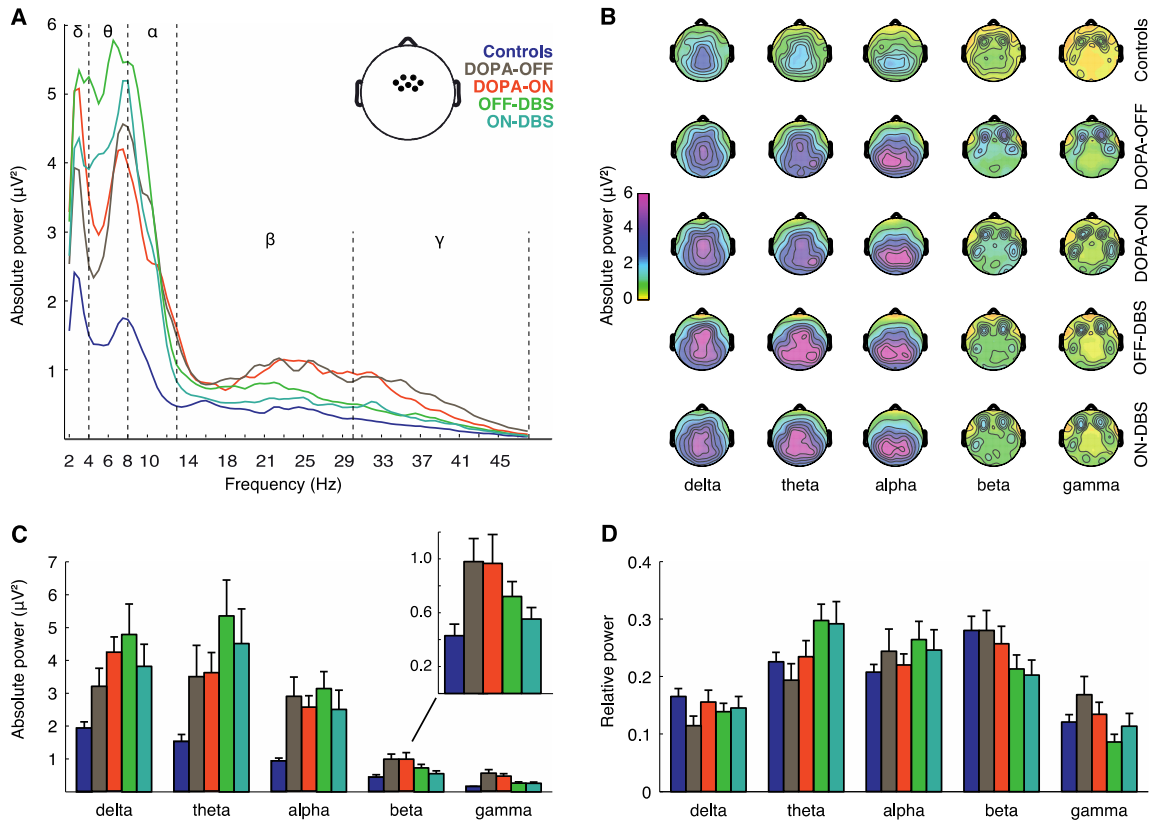

Fig. 1. Effects of treatment on resting-state EEG in the central ROI. Analysis of absolute and relative power in controls and in patients for the four therapy conditions. Absolute and relative power spectra were subdivided into five frequency bands (delta, 2–4 Hz; theta, 4–8 Hz; alpha, 8–13 Hz; beta, 13–30 Hz; gamma, 30–48 Hz). (A) Comparison of absolute power spectra. Inset, location of the seven averaged electrodes of the central ROI used for analysis of power. (B) Topographies of absolute power for controls and patient groups. (C) Absolute power in the five frequency bands. Inset, enlarged version of the distribution for absolute beta-band power. (D) Relative power in the five frequency bands. Error bars indicate SEM.

this, artifacts related to electrical stimulation within the analyzed frequency-range were still present in 5 patients. ICA components representing stimulation artifacts were clearly discernible due to their circumscribed scalp distribution involving few neighboring EEG-electrodes positioned over one or both DBS-electrodes. Furthermore, these artifacts were characterized by a highly regular and stereotypical appearance throughout the whole recording time as well as by unphysiologically sharp peaks in their activity power spectra. As a final step, outlier epoch-values were automatically detected and rejected (threshold criterion: ±100 μV).

In the present study four patients showed resting tremor. To limit the influence of tremor-related muscle artifacts, active EEG electrodes were used and statistical analyses of EEG activities were confined to the central ROI. Additionally, epochs with extensive tremor artifacts were excluded and ICA components representing tremor artifacts were removed from the EEG data. Application of this procedure ensured that for each participant at least 90% of all recorded trials could be retained.

2.7. Power spectrum analysis

A power spectrum analysis (Fast Fourier Transform) of the resting-state EEG was performed using EEGLAB. Raw data were first low-pass filtered (48 Hz), downsampled to 500 Hz and then high-pass filtered (2 Hz). A linear-phase FIR filter design using least-squares error minimization was applied. 60-point low-pass filtering was performed and the low-pass transition bandwidth was 7 Hz. For high-pass, a 750-point filtering was performed and the high-pass transition bandwidth was 0.3 Hz. This procedure minimized the contribution of movement artifacts, slow drifts (<2 Hz) and the largest part of the stimulation artifacts in the ON-DBS condition (≥130 Hz) as well as line noise (50 Hz) artifacts. Filtering and application of the above mentioned two-step procedure ensured that at least 50 s of the resting-state EEG recordings could be retained for each participant (mean: 56 ± 4 s). Mean absolute power and mean relative power were computed. Relative power is not influenced by factors such as electrode impedance, skull thickness or skin conductance. Therefore it is often preferred over absolute power representations. However, the interpretation of variations in frequency bands or group comparisons may be difficult when relying exclusively at relative power values, since frequencies in relative power are not quantified independently of each other (Pivik et al., 1993; Stoffers et al., 2007). To facilitate the evaluation of precise contributions to changes in relative power, we decided to present relative power measures in conjunction with absolute power (Pivik et al., 1993). For the relative power spectrum, we divided every bin (n = 94) of the power spectrum by the sum of the full band power (2–48 Hz). Average power was then computed separately for the 5 main frequency bands: delta (2–4 Hz), theta (4–8 Hz), alpha (8–13 Hz), beta (13–30 Hz) and gamma (30–48 Hz). In the case of absolute power, average power values for the 5 main frequency bands were computed.

To compare changes of resting-state power spectra under different conditions and in different groups, we first performed transformations towards the normal distribution for absolute and relative band power as suggested by Gasser et al. (1982): log x for absolute power and log [x / ($1 - x$)] for relative power, where x represents the absolute and the relative band power, respectively. We then performed the statistical analysis for the 5 main frequency bands. To test the variance of the five frequency bands in the different therapy conditions and groups, ANOVAs with repeated measures were performed in PASW statistics (PASW Statistics

for Mac version 18.0, SPSS Inc., Chicago, IL, USA). For interaction effects Greenhouse–Geisser corrected p-values are reported if sphericity was violated (Mauchly's sphericity test). Degrees of freedom are reported uncorrected. To test the effect of different treatments on the relative and absolute power distribution in comparison to healthy controls, four separate ANOVAs were performed for the four experimental conditions (DOPA-ON, DOPA-OFF, ON-DBS and OFF-DBS) vs. controls. The repeated measures factor Frequency-Bands had 5 levels (relative or absolute power in the five different frequency bands). Each between-subjects factor had two levels (each of the four PD-patients conditions vs. controls). To test the effect of different treatments on the relative and absolute power distribution in comparison to each other, six repeated measures ANOVAs were performed with the within-subject factors Frequency-Bands and all combinations of experimental conditions. In case of a significant main effect for Group or for Treatment (i.e., levodopa, surgery and DBS) or an interaction effect with Frequency-Bands, subsequent post-hoc analyses with regard to single band differences between Groups or Treatments were performed (two-sample t-test, pooled for comparisons between patients and control groups or paired-sample t-test for comparisons between the patients conditions). Correction for multiple comparisons is a relevant general topic concerning the analysis of non-random biological, clinical and physiological data, where real associations are to be expected and a priori hypotheses are generally formulated (Rothman, 2014). As stated in the introduction, we expect a reduction of the pathologically increased beta-band activity of PD patients following levodopa and DBS treatments. Having generated a specific hypothesis concerning the differences in resting-state EEG beta-band activity in PD patients implies that post-hoc procedures (usually used for exploratory studies, where no specific a priori hypotheses have been made), and the associated adjustments for multiple comparisons, would not strictly be necessary, as they are reducing type I errors at the expense of increasing type II errors (Field, 2009; Perneger, 1998; Rothman, 2014). Nevertheless, for both absolute and relative power, the alpha level of post-hoc analyses was conservatively Bonferroni-corrected for the 5 frequency bands (i.e., $p < 0.01$).

2.8. Time–frequency and inter-trial coherence analysis

For the analysis of spectral changes in oscillatory activity, continuous raw data were first low-pass filtered (100 Hz), downsampled to 500 Hz and then high-pass filtered (2 Hz). A linear-phase FIR filter design using least-squares error minimization was applied. 30-point low-pass filtering was performed and the low-pass transition bandwidth was 1 Hz. For high-pass, a 750-point filtering was performed and the high-pass transition bandwidth was 0.3 Hz. Artifact removal was carried out as described above. Epochs were then extracted from the continuous data starting 500 ms before click onset and lasting for 1000 ms after click onset. Baseline correction was applied in the interval from −500 ms to stimulus onset. Finally, outlier epoch-values were automatically detected and rejected setting a threshold value of ±100 μV. For each channel, time–frequency analysis was performed on frequencies from 3 to 100 Hz (step size 1 Hz) using a "Hanning" taper. Using a sliding window approach the taper (length 100 ms) was moved from −0.3 to 0.7 s in steps of 5 ms. A 100 ms time window results in a frequency resolution that is best for frequencies above 10 Hz. Since we were most interested in beta frequencies (13–30 Hz), the choice of the above-mentioned taper settings offered a good temporal resolution for this frequency of interest. Furthermore the relatively short time window of 100 ms prevented temporal smearing in the lower frequencies, which was important with respect to the short ISIs of the paradigm.

For time–frequency analyses, Fourier transformation was performed on the single-trial level prior to averaging. The resulting total power contains both signal components phase-locked and non-phase-locked to the stimulus. Power was then baseline corrected for each frequency to obtain the relative signal change: $P(t,f)_{corrected} = 100 \times (P(t,f) - P(f)_{baseline}) / P(f)_{baseline}$. The mean value across the whole epoch served as baseline. This procedure avoids the introduction of noise from the baseline into the activation period. Furthermore, an inter-trial coherence (ITC) analysis was performed by averaging the phase of the complex spectral estimates across single trials (Makeig et al., 2004; Tallon-Baudry et al., 1996). ITC is a univariate measure reflecting the phase-locking for specific frequencies at a single channel over trials. Thus, it differs from bivariate coherence measures which reflect phase-locking between two separate channels (Bruns, 2004; Herrmann et al., 2005). Values ranging from 0 to 1 indicate how the phases are distributed with respect to stimulus onset: a value of zero means complete randomly distributed phases, while a value of 1 represents a perfect phase-locking to the stimulus. Mean total power in the frequency range from 3 to 80 Hz was calculated and plotted for all experimental conditions in PD patients and for the control group. Time courses of single band power change were calculated and plotted as the mean across the frequencies from 4 to 7.5 Hz (theta), 8–12 Hz (alpha), 13–30 Hz (beta) and 31–80 Hz (gamma).

For statistical analysis in the frequency domain, we separated the rhythm conditions into two main groups: (i) rhythmic auditory stimulation presented at slow rates (1, 1.5 and 2 Hz, hereafter referred to as "slow RAS") and (ii) fast auditory pacing (4, 4.5 and 5 Hz, "fast RAS"). This subdivision was suggested by clinical observations and reports in the literature that RAS at 1–2 Hz is particularly helpful to alleviate motor impairments, especially gait disturbances, observed in PD (Enzensberger and Fischer, 1996; McIntosh et al., 1997). In contrast, auditory–motor coupling is severely impaired in response to RAS with frequencies >3 Hz (Freeman et al., 1993; Freund and Hefter, 1993; Logigian et al., 1991; Nakamura et al., 1978). Several reports in healthy participants converge on the existence of two distinct timing mechanisms for discrete (<2 Hz) and continuous (>3 Hz) movements (Huys et al., 2008; Kunesch et al., 1989; Szirmai, 2010; Toma et al., 2002). Furthermore, the change from a transient to a steady-state cortical activity, as indexed by the overlap of neuronal responses during fast auditory pacing, starts at RAS above 2 Hz (Carver et al., 2002). To avoid overlap between these two putatively distinct timing mechanisms, we excluded auditory stimulation rates between 2.5 and 3.5 Hz. Moreover, the two fastest auditory stimulation rates (5.5 and 6 Hz) were excluded from further analysis to avoid excessive overlapping of power change resettings due to the temporal proximity of auditory events and to guarantee a balanced comparison of three slow vs. three fast RAS conditions, respectively. Grouping three slow and three fast frequencies increased the trial number for each condition from 75 to 225, thus increasing the statistical power for the analyses. Moreover, this approach reduced the number of tests between auditory stimulation conditions, minimizing the probability of type-I statistical errors. Note that the epochs defined here (from −0.2 to 0.5 s relative to stimulus onset) are often longer than the inter-stimulus intervals (ISI) and thus contain responses to more than one stimulus. This is particularly relevant for the "fast RAS" group containing auditory pacing frequencies up to 5 Hz (i.e., with an ISI interval of 200 ms). Two adjacent peri-stimulus time-windows were considered for non-parametric cluster-based statistical analysis. A pre-stimulus time-window ranging from −80 to 0 ms (stimulus onset), and a post-stimulus time-window from 0 ms (stimulus onset) to 80 ms were tested separately for pre- and post-stimulus intervals. Together, both intervals had a length of 160 ms, which is shorter than the ISI of the fastest RAS condition considered (i.e., 5 Hz, 200 ms ISI).

Cluster-based non-parametric randomization tests were performed for mean values of power and ITC between groups (Controls vs. DOPA-OFF and Controls vs. ON-DBS) and between conditions (DOPA-ON vs. DOPA-OFF and ON-DBS vs. DOPA-OFF). These tests control the type I error rate in experimental designs involving multiple comparisons by clustering adjacent time–frequency points exhibiting the same effect (cluster $\alpha = 0.05$, 1000 randomizations; Maris and Oostenveld, 2007). Results of power differences between groups and conditions were plotted as z-scores and significant clusters with p-values < 0.05 were highlighted. Differences in the beta-band power and ITC as a

function of time (between groups and between experimental conditions) were tested performing cluster-based non-parametric analyses of the sampling points of the curves as described above. We applied two-sample t-tests, pooled for comparisons between patients and control groups and paired-sample t-tests for comparisons between the different experimental conditions in patients, respectively.

Table 2
Repeated measures ANOVA for effects of treatment and group on resting-state EEG.

Repeated measures ANOVA	Factors			Interaction of factors			p-values of post-hoc analyses for:				
	df	f	p	df	f	p	Delta	Theta	Alpha	Beta	Gamma
Relative power											
DOPA-OFF vs. DOPA-ON											
Frequency-Bands	4,44	3.787	.048	4,44	3.416	.050	**.006**	.044			
Levodopa	1,11	4.374	.060								
DOPA-OFF vs. OFF-DBS											
Frequency-Bands	4,44	6.547	.005	4,44	8.779	.003		<**.001**		.027	.017
Surgery	1,11	.297	.597								
DOPA-OFF vs. ON-DBS											
Frequency-Bands	4,44	3.831	.039	**4,44**	**13.115**	<**.001**	**.008**	<**.001**		**.002**	**.006**
Surgery	1,11	.086	.775								
DOPA-OFF vs. controls											
Frequency-Bands	**4,88**	**9.217**	<**.001**	4,88	1.178	.317	.015				
Group	1,22	7.139	.014								
DOPA-ON vs. OFF-DBS											
Frequency-Bands	**4,44**	**9.435**	**.001**	4,44	3.845	.034		.018			
Surgery	1,11	3.511	.088								
DOPA-ON vs. ON-DBS											
Frequency-Bands	4,44	5.345	.013	4,44	2.625	.047		.041		.015	
Surgery	1,11	3.543	.087								
DOPA-ON vs. controls											
Frequency-Bands	**4,88**	**12.319**	<**.001**	4,88	.180	.842					
Group	1,22	4.454	.046								
OFF-DBS vs. ON—DBS											
Frequency-Bands	**4,44**	**9.527**	<**.001**	4,44	.979	.404					
DBS	1,11	.348	.567								
OFF-DBS vs. controls											
Frequency-Bands	**4,88**	**22.819**	<**.001**	4,88	3.335	.014		.037			.049
Group	1,22	8.709	.007								
ON-DBS vs. controls											
Frequency-Bands	**4,88**	**12.574**	<**.001**	4,88	1.640	.195				.034	
Group	1,22	6.414	.019								
Absolute power											
DOPA-OFF vs. DOPA-ON											
Frequency-Bands	**4,44**	**29.383**	<**.001**	4,44	3.423	.053	.016				
Levodopa	1,11	.600	.455								
DOPA-OFF vs. OFF-DBS											
Frequency-Bands	**4,44**	**43.843**	<**.001**	4,44	8.625	.005	.013	**.003**			.037
Surgery	1,11	.584	.461								
DOPA-OFF vs. ON-DBS											
Frequency-Bands	**4,44**	**30.879**	<**.001**	**4,44**	**14.752**	<**.001**				**.008**	**.008**
Surgery	1,11	2.391	.150								
DOPA-OFF vs. controls											
Frequency-Bands	**4,88**	**71.830**	<**.001**	4,88	1.122	.335	.050	.030	**.002**	**.006**	**.003**
Group	**1,22**	**18.627**	<**.001**								
DOPA-ON vs. OFF-DBS											
Frequency-Bands	**4,44**	**70.890**	<**.001**	4,44	3.535	.049		.038			
Surgery	1,11	.045	.836								
DOPA-ON vs. ON-DBS											
Frequency-Bands	**4,44**	**49.447**	<**.001**	4,44	2.492	.105				**.002**	.020
Surgery	1,11	11.963	.005								
DOPA-ON vs. controls											
Frequency-Bands	**4,88**	**122.296**	<**.001**	4,88	.192	.837	<**.001**	**.001**	<**.001**	**.010**	**.005**
Group	**1,22**	**24.134**	<**.001**								
OFF-DBS vs. ON-DBS											
Frequency-Bands	**4,44**	**64.007**	<**.001**	4,44	1.108	.350			.039	.025	
DBS	1,11	4.339	.061								
OFF-DBS vs. controls											
Frequency-Bands	**4,88**	**176.203**	<**.001**	4,88	3.035	.021	**.002**	<**.001**	<**.001**	.021	.018
Group	**1,22**	**20.167**	<**.001**								
ON-DBS vs. controls											
Frequency-Bands	**4,88**	**120.963**	<**.001**	4,88	1.423	.249	.026	**0.009**	.022		.044
Group	1,22	9.359	.006								

The reported values are degrees of freedom (df), F- and p-values for all the performed repeated measures ANOVA for both relative and absolute power changes. The within-subjects factors are Frequency-Bands (delta, theta, alpha, beta, gamma) and Treatment (Levodopa, Surgery, DBS). The between-subjects factor is Group (patients vs. controls). Results of the repeated measures ANOVA with p values still significant after Bonferroni corrections for the 20 separate ANOVAs are highlighted in bold (i.e., $p < 0.0025$), while results with p-values between ≥0.05 and ≤0.06 are reported in underlined font. If significant effects of factor Treatment or significant interactions between factor Treatment and factor Frequency-Bands were found in the ANOVA, post-hoc p-values for t-test comparisons between single frequency bands are reported. For post-hoc tests, p-values still significant after Bonferroni corrections are reported in bold (i.e., $p < 0.01$).

3. Results

3.1. Effects of levodopa and STN-DBS on resting-state EEG

To test whether cortical activity was influenced by experimental conditions in the absence of sensory stimulation, we first investigated possible effects of levodopa and STN-DBS on absolute and relative spectral power of the resting-state EEG (Fig. 1). We focused on spectral power recorded in the central ROI, since this region showed the most pronounced EEG-activity modulation in response to the RAS. Specifically, we intended to characterize beta-band resting-state power changes in this ROI in regard to the different treatments. To this end, we performed repeated-measures ANOVA with between-subjects factor Group (patients vs. controls) and within-subjects factors Frequency-Bands (delta, theta, alpha, beta, gamma) and Treatment (DOPA-OFF, DOPA-ON, OFF-DBS, ON-DBS). Table 2 summarizes the results of the ANOVA analysis for both relative and absolute power. Relative power measures are displayed in conjunction with absolute power to ensure an accurate evaluation of contributions to changes in relative power (Pivik et al., 1993). Adjusting statistical significance for the number of tests that have been performed is recommended to control for type I errors (i.e., detecting an effect that is not present). Unfortunately, this procedure is often inflating type II errors (i.e., truly important differences are deemed non-significant) and thus missing real differences (Perneger, 1998; Rothman, 2014, 1990). Therefore, we report here the uncorrected results, as suggested by a number of statisticians (Bender and Lange, 2001; Perneger, 1998; Rothman, 2014, 1990; Saville, 1990; Savitz and Olshan, 1995). Highlighted are p-values, which would survive most conservative Bonferroni corrections (i.e., p-values < 0.0025 for the 20 separate ANOVAs reported in Table 2 are marked in bold, and p-values < 0.00625 for the 8 power changes comparisons reported in Fig. 3 are marked with an asterisk). It should be noted that all post-operative recordings took place after overnight withdrawal of anti-parkinsonian medication.

3.1.1. Relative power changes

For relative power we consistently found main effects of Frequency-Bands and Group (patients vs. controls, Fig. 1D and Table 2). The interaction between Frequency-Bands and Group reached significance in the comparison OFF-DBS vs. controls. Significant interaction effects between Frequency-Bands and Treatment were found in the comparison of the two pre-operative conditions DOPA-OFF and DOPA-ON with the two post-operative conditions OFF-DBS and ON-DBS. Compared to the pre-operative baseline measurement in the absence of dopaminergic medication (DOPA-OFF), a significant increase of relative power in the theta frequency band was observed for patients in both post-operative conditions (see Fig. 1D). Notably, a significant reduction of relative power in the beta and gamma frequency range was observed for the post-hoc comparison DOPA-OFF vs. ON-DBS, pointing to a DBS-induced reduction of cortical high-frequency power (see Fig. 1D).

In summary, after DBS surgery a shift of relative power from beta and gamma frequencies towards theta was evident in the group of PD patients.

3.1.2. Absolute power changes

In a similar vein, analysis of absolute power revealed main effects of Frequency-Bands and Group (patients vs. controls), and a significant interaction of factors Frequency-Bands and Group for the

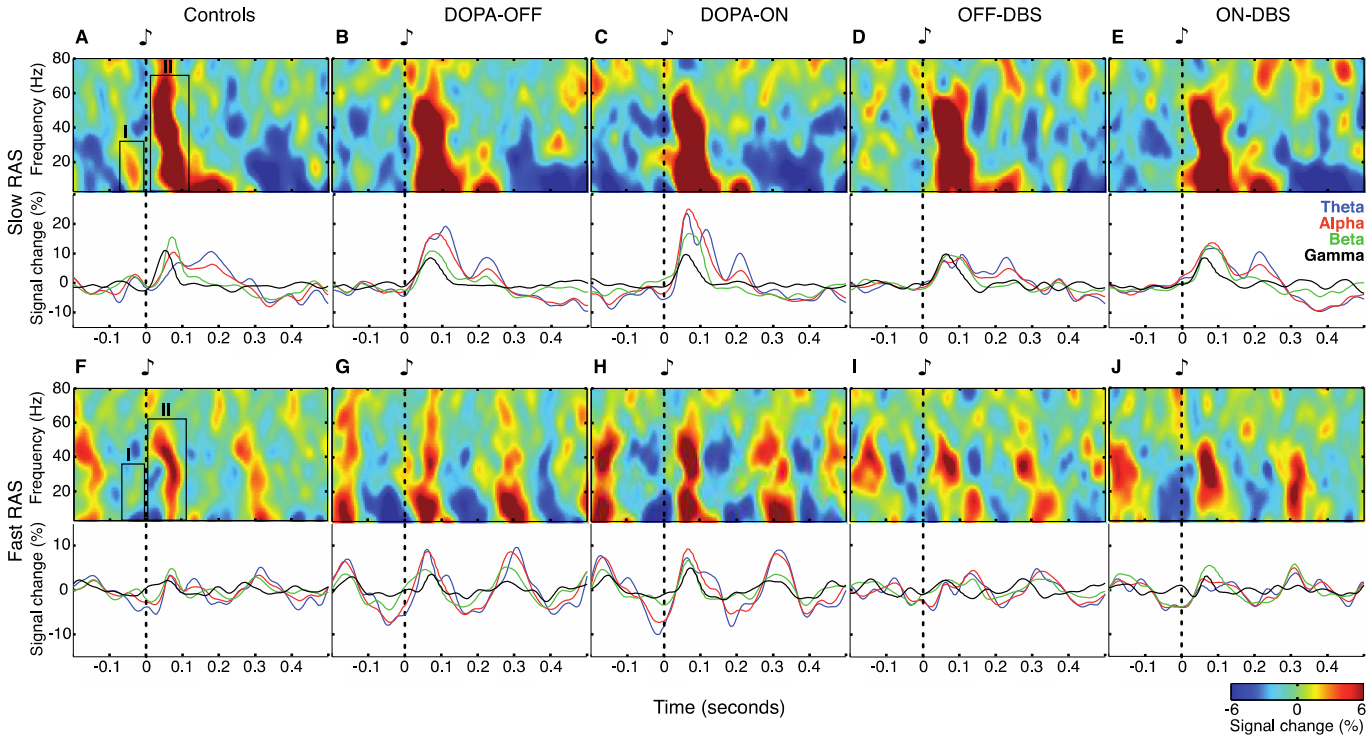

Fig. 2. Mean total power and power time courses. (A–E) Effects of slow RAS on total power in controls and in patients for the four therapeutic conditions. Top panels show time–frequency plots of the total power averaged across rhythmic auditory stimulation at 1, 1.5 and 2 Hz. Two peri-stimulus response components were identified in mean total power (A): (I) pre-stimulus power increase involving in particular beta frequencies (13–30 Hz, −70–0 ms); (II) an early power increase (4–80 Hz, 0–120 ms). Bottom panels show peri-stimulus total power time courses for the theta-, alpha-, beta- and gamma-band. (F–J) Effects of fast RAS on total power. Top panels show time–frequency plots of the total power averaged across rhythmic auditory stimulation at 4, 4.5 and 5 Hz. Boxes in (F) indicate the same two response components as in (A). Bottom panels show peri-stimulus total power time courses. The "fast RAS" group contains auditory pacing frequencies up to 5 Hz, i.e., with an inter-stimulus interval (ISI) of 200 ms. Note that the epochs plotted here are longer than ISIs for the "fast RAS" condition and thus contain responses to more than one stimulus. All time–frequency plots and power time courses display signal change (in %) relative to the average across the entire data epoch.

comparison OFF-DBS vs. controls. PD patients constantly displayed higher absolute power values than controls across all frequency bands — except for beta-band activity in the comparison between controls and patients ON-DBS (Fig. 1A, C and Table 2). Furthermore, and in line with the results on relative power, significant interactions of factors Frequency-Bands and Treatment were found in the comparisons DOPA-OFF vs. OFF-DBS and ON-DBS, as well as DOPA-ON vs. OFF-DBS. In line with the results on relative power, post-hoc tests comparing absolute power between DOPA-OFF vs. OFF-DBS showed a significant increase in theta-band power for patients OFF-DBS. When directly comparing DOPA-OFF to ON-DBS, absolute beta and gamma power was significantly reduced in the ON-DBS condition. A similar reduction of absolute beta power with ON-DBS was also found in the post-hoc comparisons with the DOPA-ON condition. Notably, beta power in the ON-DBS condition was reduced compared to the OFF-DBS condition in the post-hoc contrast between ON-DBS vs. OFF-DBS ($p = 0.025$; see inset of Fig. 1C). However, this difference did not survive a conservative Bonferroni correction (i.e., $p < 0.01$).

Taken together, after surgery an increment of theta power with DBS switched OFF was observed in PD patients. Importantly, STN-DBS suppressed high-frequency activities and lowered in particular beta-band oscillatory power to control level.

3.1.3. Reliability of resting-state power recordings

The topographical patterns of absolute power in the EEG were similar for all frequency bands, irrespective of group or experimental condition (Fig. 1B). The finding of consistent scalp topographies for resting-state activity before and after surgery — as well as in comparison with the control group — argues against a significant impact of DBS-artifacts and/or component rejections in our study. We cannot categorically exclude possible contributions from undetected DBS-artifact activity, but believe that the results reported here were not significantly biased by our careful artifact-removal procedure.

In order to investigate a possible influence of resting tremor on ongoing theta-band activity, we correlated absolute EEG theta power with the corresponding tremor power values as derived from simultaneous accelerometry recordings. To this end, we performed a spectral analysis (Fast Fourier Transform, same settings as for EEG analysis) for the accelerometer signals. Average tremor power values between 4 and 8 Hz were then computed for the two conditions DOPA-OFF and OFF-DBS, in the absence of anti-parkinsonian medication. Due to the non-normal distribution of tremor and theta power values (Shapiro–Wilk Test, alpha level = 0.05), p and rho values were calculated using non-parametric Spearman's correlations. Tremor power values did not correlate with theta-band power in the EEG, neither in the pre-operative condition DOPA-OFF ($rho = -0.08$; $p = 0.82$) nor in the post-operative condition OFF-DBS ($rho = -0.45$; $p = 0.14$). A direct comparison of tremor power between these two pre- and post-operative conditions did not show significant differences ($W(11) = 25$; 0.30; Wilcoxon signed rank test). To stay in line with the methods applied before in other studies of resting-state EEG in Parkinson's disease (Bosboom et al., 2006; Silberstein, 2005; Stoffers et al., 2007), we correlated absolute theta power values also with the corresponding tremor sub-scores in the motor subsection of the UPDRS (UPDRS part III, sum of items 20 and 21) of conditions DOPA-OFF (mean score 3.8 ± 3.9) and OFF-DBS (mean score 5.1 ± 3.1). UPDRS tremor scores did not correlate with theta-band power in the EEG, neither in the DOPA-OFF ($rho = 0.21$; $p = 0.51$) nor in the OFF-DBS condition ($rho = 0.31$; $p = 0.38$).

Consequently, it is improbable that tremor artifacts accounted for the observed post-operative theta power increase in the EEG, in accordance with previous results reported by Bosboom et al. (2006) and Stoffers et al. (2007).

3.2. Time–frequency analysis of event-related power changes and inter-trial coherence

3.2.1. Evoked and induced oscillations

Oscillatory signals can be defined by their amplitude and phase. Evoked oscillations are phase-locked to the stimuli, i.e., they reflect those components of the oscillatory signal whose phase is similar after every stimulus presentation. Evoked power can be considered as the frequency-domain equivalent of the event-related potential. In contrast, induced neuronal oscillations are not phase-locked to stimulus onset. We first carried out a time–frequency analysis of event-related changes in total power (Fig. 2), which comprises both induced and evoked oscillatory components. In order to disentangle which parts of the power responses are phase-locked to the stimuli, we analyzed inter-trial coherence (ITC; Fig. 4).

In the following paragraphs and figures, time–frequency analysis results will be presented in succession, first for slow and then for fast RAS.

3.2.2. Total power changes during slow RAS

During slow RAS, two distinct peri-stimulus components could be differentiated in the EEG total power for healthy control participants (labeled I and II in Fig. 2A). (I) From −70 to 0 ms *before* stimulus onset, low-frequency oscillations — mainly in the beta-band — displayed a local peak. As illustrated by the line plot graphs in Fig. 2B–E, this pre-stimulus beta-power modulation was absent in all conditions in PD patients. (II) Immediately after stimulus onset, a phasic broad-band (4–80 Hz) power increase was evident, rapidly decaying within the first 120 ms. The duration of this broad-band peak was considerably increased (for ~50 ms) in PD patients (Fig. 2B–E). Irrespective of levodopa treatment, post-stimulus theta and alpha power was excessively high in patients before surgery (Fig. 2B and C) compared to post-operative recordings (Fig. 2D and E) or healthy controls (Fig. 2A). Cluster-based statistic of event-related power changes revealed pre-stimulus differences — mainly within the beta-band — for contrasts between patients in DOPA-OFF and ON-DBS vs. controls (cluster randomization test, $p = 0.016$ and $p = 0.019$, respectively; upper panels of Fig. 3A and D).

3.2.3. Time courses of beta-band total power during slow RAS

As oscillatory activity in the beta-band (13–30 Hz) has repeatedly been postulated to play an important role in rhythm perception and audio-motor integration, we thoroughly examined changes in this particular frequency band and visualized its modulation profile as line plots in bottom panels of Fig. 3A–D. The most salient power difference between patients and controls during slow RAS was consistently found shortly before stimulus onset. This increase of beta oscillatory activity preceding stimulus onset was absent in patients (Fig. 3A and D). In the control group, auditory beta power modulation displayed a stereotypical triphasic profile (see line plots in lower panels of Fig. 3A and E). A pre-stimulus beta power increase (−70–0 ms), returning to baseline levels around stimulus onset was followed by a post-stimulus beta power increase (20–100 ms). While controls showed a clear beta peak shortly (~40 ms) before stimulus onset during slow RAS (marked by an arrowhead bottom panels of Fig. 3), this pre-stimulus beta modulation was absent in patients in DOPA-OFF (cluster randomization test, $p = 0.005^*$) and ON-DBS (cluster randomization test, $p = 0.015$). Note that the post-stimulus beta modulation profile during slow RAS was largely similar between the two groups. Moreover, the contrast between the two post-operative conditions (ON versus OFF-DBS) was statistically not significant.

3.2.4. Inter-trial coherence (ITC) during slow RAS

Fig. 4 depicts the phase-locking across trials as reflected in ITC values. According to this ITC analysis, only the second (post-stimulus) component of the two previously described response components contained phase-locked oscillatory activity (Fig. 4, upper panels A–E). The early power increase (component II, 0–120 ms) was phase-locked

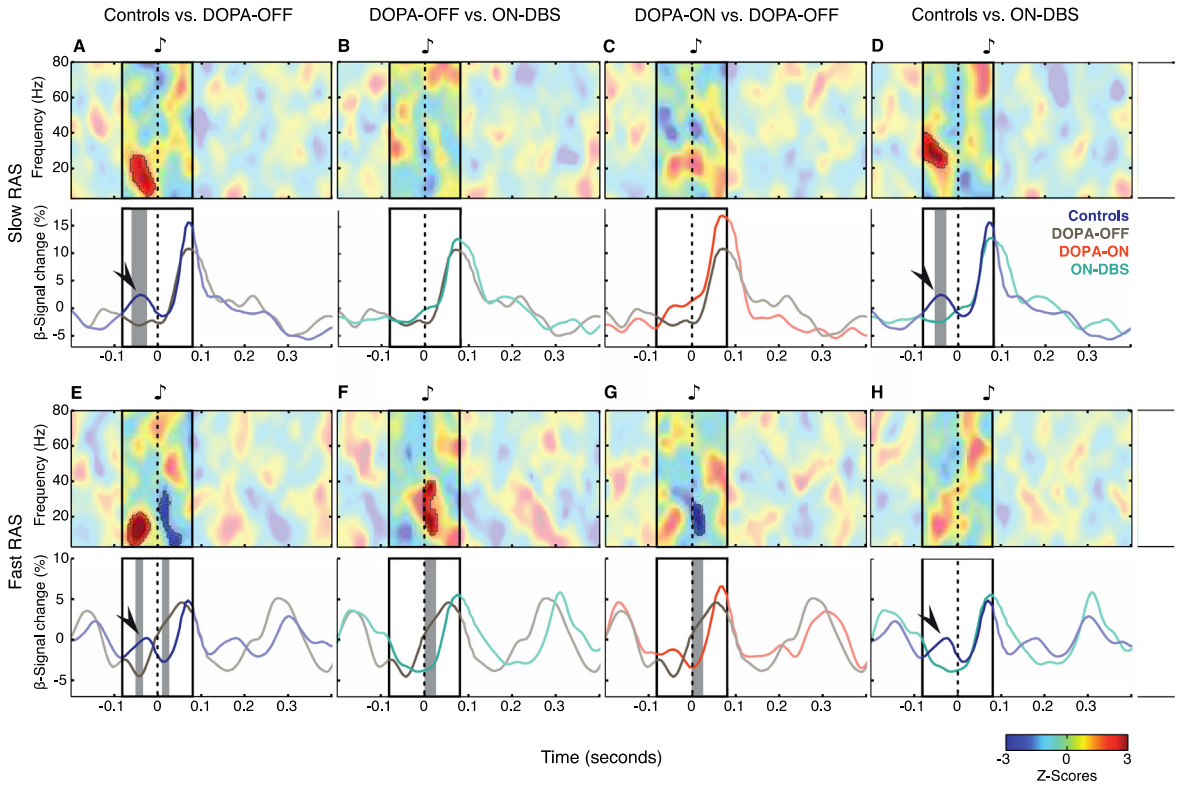

Fig. 3. Mean differences and time courses of beta-band total power. (A—H, top panels) Mean power differences at slow RAS (auditory stimulation at 1, 1.5 and 2 Hz) and fast RAS (auditory stimulation at 4, 4.5 and 5 Hz). Unmasked regions in the plots show significantly different z-score clusters (A—H, bottom panels). Time courses of beta-band power at slow and fast RAS. Arrowheads indicate the pre-stimulus beta power increase (−70–0 ms) observed in controls. Gray shaded areas in the bottom panels show significantly different beta-band changes. The "fast RAS" group contains auditory pacing frequencies up to 5 Hz, i.e., with an inter-stimulus interval (ISI) interval of 200 ms. Note that the epochs plotted here are longer than ISIs for the "fast RAS" condition and thus contain responses to more than one stimulus. The peri-stimulus frames marked in the panels represent the time interval used for statistical testing of differences of event-related power changes for the entire considered frequency range (3–80 Hz; upper panels) and for beta-power time courses (for details see methods section). Testing was confined to this time interval to avoid overlapping with preceding or successive stimulus events. All time–frequency plots and power time courses display signal change (in %) relative to the average across the entire data epoch.

across all frequencies and in particular in the gamma-frequency range around 40 Hz. In contrast, component I — representing a pre-stimulus increase of beta power (13–30 Hz, −70–0 ms) — was clearly not phase-locked to the stimulus and may therefore reflect an intrinsically generated oscillatory process. Cluster-based statistical analysis of the two peri-stimulus components did not show any significant ITC-difference for the abovementioned contrasts, neither in the whole frequency range (3–80 Hz), nor in the more specific analysis of temporal profiles of beta-band power (cluster randomization tests, $p > 0.05$; data not shown).

3.2.5. Total power changes during fast RAS

At fast RAS, response modulations of the previously described total power response components were still apparent but generally less distinct and of lower magnitude compared to responses during slow auditory pacing (upper panels of Fig. 2F–J). Notably, a pre-stimulus beta power increase was still present in healthy control subjects (component I in Fig. 2F), but this peak was never observed in PD patients. (II) Post-stimulus amplitude modulation was still dominated by a broad-band power increase in both patients and controls, albeit of shorter duration and smaller magnitude compared to slow RAS. Similar to slow RAS, periodic entrainment of theta-, alpha- and beta-power by fast RAS was especially pronounced before DBS surgery (Fig. 2G and H). In the post-operative conditions, the overall response modulation level was in the same range as for healthy participants. In particular, the low-frequency content of the dominant broad-band power increase (component II) was much reduced during fast auditory pacing following DBS surgery (Fig. 2I and J). Cluster-based statistics of event-related power changes revealed a significant pre-stimulus deficiency of power predominantly in the beta-band in PD patients in DOPA-OFF when compared to controls (cluster randomization test, $p = 0.006^*$; upper panel of Fig. 3E). Post-stimulus differences in the beta-band were significant in the contrasts controls vs. DOPA-OFF (cluster randomization test, $p = 0.034$; upper panel of Fig. 3E), DOPA-OFF vs. ON-DBS (cluster randomization test, $p = 0.013$; upper panel of Fig. 3F) and DOPA-ON vs. DOPA-OFF (cluster randomization test, $p = 0.04$; upper panel of Fig. 3G).

3.2.6. Time courses of beta-band total power during fast RAS

The specific temporal dynamics of beta-band responses during fast RAS also displayed significant differences between patients and controls. For patients OFF medication, the periodic beta power fluctuations after stimulus onset appeared to be shifted ahead in time when compared to controls, DOPA-ON and ON-DBS (see line plots in Fig. 3E–G). Furthermore, the duration of these stimulus-induced beta peaks were significantly longer in patients OFF medication (peak width at half height, 106 ms) compared to controls (peak width, 46 ms; cluster randomization test, $p = 0.027$). A slight beta decrease, which characterized the power fluctuation immediately before stimulus onset in control subjects, was replaced by gradual ramping of beta power across stimulus onset in patients without levodopa (cluster randomization test, $p = 0.045$). Interestingly, both dopaminergic medication and DBS normalized the time course and peak duration of stimulus-driven beta power fluctuations in the fast RAS condition. This is illustrated by significant differences of beta power line plots for DOPA-ON compared to DOPA-OFF (Fig. 3G; cluster randomization test, $p = 0.001^*$) and ON-DBS compared to DOPA-OFF (Fig. 3F; cluster randomization test, $p = 0.003^*$). There was no longer a statistical difference between controls

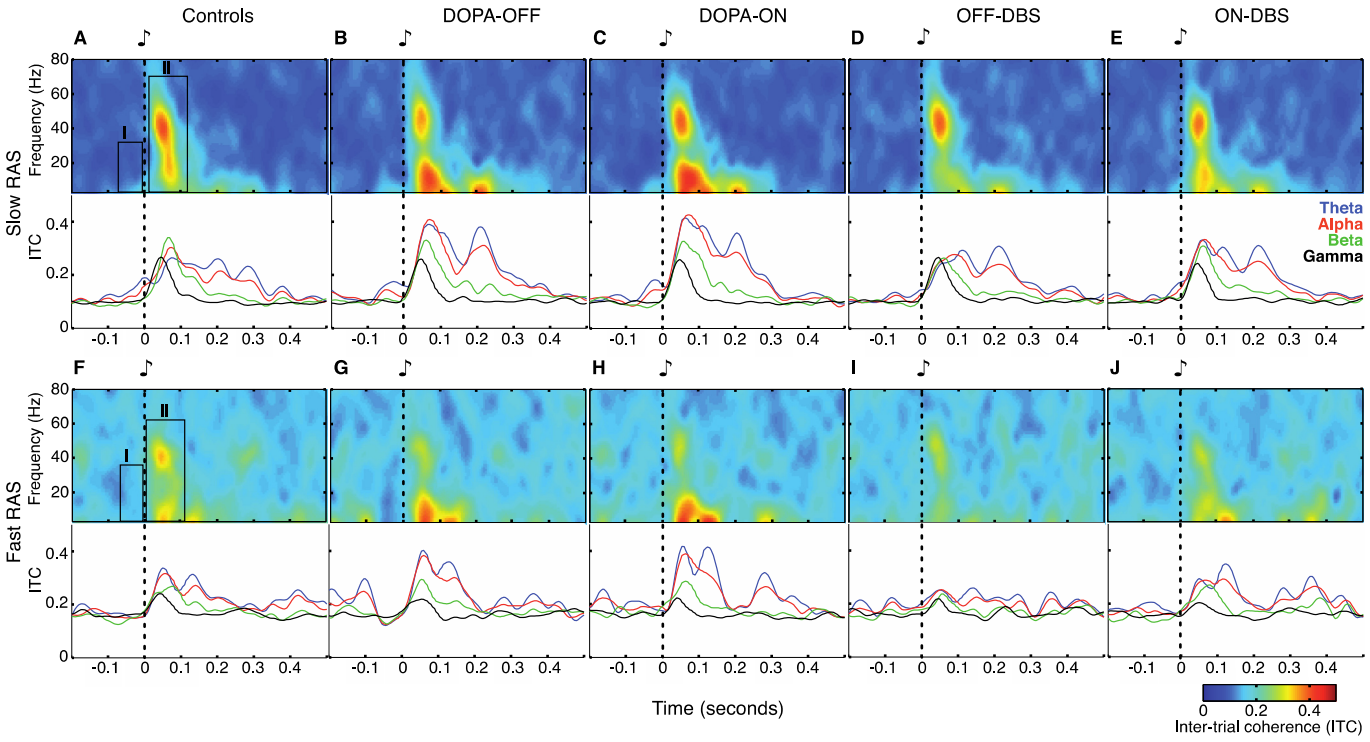

Fig. 4. ITC spectral characteristics and time courses. (A–E) Effects of slow RAS on ITC in controls and in patients for the four therapy conditions. Top panels show time–frequency plots of the ITC computed across all trials with auditory stimulation at 1, 1.5 and 2 Hz. The boxes in the upper panels of (A) indicate the position of the two power-response components as described in Fig. 2. Bottom panels show ITC courses for the theta-, alpha-, beta- and gamma-band. Note that only response component II shows phase-locking to the stimulus. (F–J) Effects of fast RAS on ITC. Top panels show time–frequency plots of the ITC computed across all trials with auditory stimulation at 4, 4.5 and 5 Hz. Boxes in (F) indicate the same two response components as in (A). Bottom panels show ITC time courses. The "fast RAS" group contains auditory pacing frequencies up to 5 Hz, i.e., with an inter-stimulus interval (ISI) of 200 ms. Note that the epochs plotted here are longer than ISIs for the "fast RAS" condition and thus contain responses to more than one stimulus. This also explains the higher baseline offset for fast RAS (0.2) than for slow RAS (0.1), since the mean ITC-value across the whole epoch served as baseline.

and patients with PD ON-DBS (Fig. 3H). Note that in the fast RAS condition, the pre-stimulus beta-band increase was still absent for patients with DBS-ON (Fig. 3H). No statistical significant difference was found for the comparison between OFF- and ON-DBS in the processing of fast RAS.

3.2.7. Inter-trial coherence (ITC) during fast RAS

ITC analysis revealed that, as for the slow RAS condition, the pre-stimulus beta-modulation observed in control participants (component I) was not phase-locked to the auditory stimuli in PD patients. As for the slow RAS condition, cluster-based statistical analysis of the peri-stimulus components did not show any significant ITC-difference for the considered contrasts, neither when examining the whole frequency range (3–80 Hz), nor for the temporal profiles of beta power (cluster randomization tests, $p > 0.05$; data not shown).

3.2.8. Interrelation between pre- and post-stimulus oscillatory activities

To test the interaction between pre- and post-stimulus beta-band oscillatory activities in controls and in patients for the four therapeutic conditions, correlations of pre- and post-event mean values of beta-band activities were calculated. Mean beta power as well as mean ITC values were computed for the two adjacent intervals considered for the peri-stimulus statistical analysis (i.e., a pre-stimulus time-window from −80 to 0 ms, and a post-stimulus time-window from 0 to 80 ms). Due to the non-normal distribution of beta power values (Shapiro–Wilk Test, alpha level = 0.05), p and rho values were calculated using non-parametric Spearman's correlations.

For slow RAS pre-stimulus beta power values did not correlate with post-stimulus beta power values, neither in controls (rho = −0.07; p = 0.83), nor in the four therapeutic conditions DOPA-OFF (rho = −0.21; p = 0.51), DOPA-ON (rho = −0.18; p = 0.57), OFF-DBS (rho = 0.02; p = 0.96), ON-DBS (rho = 0.24; p = 0.44). Notably, for the fast RAS instead, significant *negative* correlations were found in controls (rho = −0.67; p = 0.020), in patients in DOPA-OFF (rho = −0.71; p = 0.012) and in ON-DBS (rho = −0.70; p = 0.014). Patients in DOPA-ON (rho = −0.50; p = 0.099) and in OFF-DBS (rho = −0.49; p = 0.10) exhibited a negative correlation trend between pre- and post-stimulus beta power that did not reach significance.

As for beta-band power, at slow RAS pre-stimulus beta-band ITC values did not correlate with post-stimulus beta-band ITC values, neither in controls (rho = 0.20; p = 0.53), nor in the four therapeutic conditions DOPA-OFF (rho = −0.21; p = 0.51), DOPA-ON (rho = −0.34; p = 0.29), OFF-DBS (rho = −0.37; p = 0.24), ON-DBS (rho = −0.10; p = 0.77). Also at fast RAS, no significant correlations between pre- and post-stimulus beta-band ITC values were observed — neither in controls (rho = −0.21; p = 0.51), nor in the four therapeutic conditions DOPA-OFF (rho = 0.14; p = 0.67), DOPA-ON (rho = =0.09; p = 0.78), OFF-DBS (rho = −0.37; p = 0.24), and ON-DBS (rho = 0.36; p = 0.26).

From this correlation analysis we can exclude carry over effects between pre- and post-event beta-band activities due to the temporal resolution of time frequency analysis and the temporal proximity of events. In such a case we would have expected significant *positive* correlations between pre- and post-stimulus beta activities, but this case was never observed.

Importantly, both the ITC analysis and the absence of any correlation between pre- and post-stimulus beta-band ITC values, suggest that the pre-stimulus beta-modulation in control persons was not phase-locked to the auditory stimuli, and thus the reported pre-stimulus differences are due to changes in intrinsically generated beta-band power.

4. Discussion

In this study, we have investigated the effects of dopaminergic medication and high-frequency STN-DBS on resting-state EEG-activity and

on dynamics of EEG-responses to slow and fast RAS with a specific focus on oscillatory activity in the beta frequency range. Here, we provide the first evidence for deficient sensory processing of rhythmic auditory stimuli in patients with PD that is both tempo-dependent and sensitive to neuromodulatory treatment. First, chronic STN-DBS led to a reduction of cortical beta-band power in the resting-state, thus providing further support for a specific influence of STN-DBS on cortical beta activity. Second, in response to RAS beta-band power was consistently peaking shortly before stimulus onset in healthy subjects, which was never observed in PD patients. In the patients group the post-stimulus beta amplitude modulation was also highly abnormal. We could demonstrate that dopaminergic medication and STN-DBS restored a normalized beta modulation profile in patients during fast RAS, possibly reflecting alleviations of Parkinsonian symptoms with movement at faster rhythms.

4.1. Limitations of the approach

It is conceivable that surgery-related skull defects such as incompletely sealed burr holes may have resulted in a distorted spread of scalp EEG signals (Litvak et al., 2011; Oostenveld and Oostendorp, 2002). As discussed elsewhere in detail (Gulberti et al., 2015), in our study we did not observe topographical changes nor local enhancements of signal amplitude, which might be expected to emerge from skull defects. A further source of concern about perioperative EEG recordings may be related to the "stun" effect, a temporary post-operative amelioration of parkinsonism due to microlesions as a consequence of electrode implantation (Eusebio and Brown, 2009). Stun effects are of rather short duration and typically disappear within 1 month after surgery (Jech et al., 2012). In line with these reports, post-operative UPDRS-III scores in the OFF-DBS condition (assessed 3–5 months following surgery in the DOPA off state at time of recordings) were not significantly different from baseline pre-operative UPDRS-III scores (respectively 40 ± 10 and 34 ± 12; [$t(9) = -1.66$; $p = 0.13$], paired t-test). In fact, the slightly increased UPDRS-score argues against residual effects of surgery-related microlesions. Nevertheless, long-term carry-over effects of chronic high-frequency DBS may explain the lack of significant differences in the contrasts between the two post-operative conditions (ON versus OFF-DBS) in the processing of slow and fast RAS. Switching off the stimulator for 30 min was probably not sufficient to reestablish the pre-operative pathological oscillation activity. Indeed, at least 3 h OFF-DBS are required to estimate the whole clinical effect of stimulation (Temperli et al., 2003).

The results of modulation effects of levodopa and DBS on the electrophysiological profile of PD patients could have been partially influenced by the standard procedure applied to test PD patients in the condition of levodopa withdrawal. For medical and ethical reasons, medication is usually suspended only during the night before the experimental recordings (for ~12 h). But this period of time is probably too short to reach a genuine dopa-off state, since the clinical effects of dopamine agonists and dopamine degrading inhibitors, which are frequently combined with levodopa treatment, are lasting for several days (Ahlskog et al., 1994; Blin, 2003). Thus, long-term carry-over effects of anti-parkinsonian medication could not be completely excluded as a factor possibly influencing the electrophysiological profile of PD patients.

Given the temporal proximity of the events in the fast RAS to the oscillatory responses, some pre-stimulus oscillatory activity could potentially be also represented in the post-stimulus activity and vice versa. The local maxima and minima (i.e., the peaks of the power activity) are not shifted by the time–frequency analysis methods. As evidenced in Fig. 3A and E, in controls the pre–post-event beta peaks are clearly separated by a local minima centered around the event, thus minimizing the probability of temporal smearing between these two separate components. Moreover, in patients the pre-stimulus beta is absent and the peak of post-stimulus beta activity is occurring at about 80 ms after stimulus, thus temporally distinct from pre-stimulus activities. Additionally, since all conditions and groups were analyzed with the same time–frequency settings, the significant differences between beta modulations in the different groups or conditions are still reliable, since equally influenced by the temporal resolution of time–frequency analysis applied. In conclusion, from the results of the correlations between pre- and post-event mean values of beta-band activities we can exclude carry over effects between pre- and post-event beta-band activities. In such a case we would have expected significant positive correlations between pre- and post-stimulus beta activities, but this case was never observed.

4.2. Resting-state spectral characteristics

We first addressed the question of possible effects of neuromodulatory interventions on resting-state oscillatory dynamics, particularly focusing on the beta-band. One principal finding was an enhancement of absolute power across a broad range of frequencies in patients with PD compared to healthy controls. This global increase of absolute power in PD patients is in agreement with previous reports (Moazami-Goudarzi et al., 2008; Tanaka et al., 2000), which attributed this effect to a pathophysiological chain reaction initiated by the effects of dopamine denervation on BG-thalamo-cortical circuitries. In this concept, thalamo-cortical dysrhythmia (TCD), characterized by a pathological increase of low-frequency oscillatory bursting in thalamo-cortical modules, leads to a pathological augmentation of low- and high-frequency activities in the EEG (Moazami-Goudarzi et al., 2008).

To the best of our knowledge, the finding that theta-band power is increased in patients after DBS surgery is new. Slowing of EEG activity in comparison to healthy subjects is a consistent finding in patients with PD (Soikkeli et al., 1991; Stoffers et al., 2007), and increased theta power has been associated with clinical measures of disease progression (Bosboom et al., 2006; Serizawa et al., 2008; Soikkeli et al., 1991; Stoffers et al., 2007) and cognitive decline, respectively (Neufeld et al., 1994, 1988; Olde Dubbelink et al., 2013; Sinanović et al., 2005; Tanaka et al., 2000). It cannot be decided with certainty whether the observed theta increase after DBS surgery was related to progression of motor symptoms or reduced cognitive functions, as the latter were not specifically assessed in this study. However, it is of note that the mean patient's postoperative UPDRS-III motor performance OFF-DBS was only slightly worse compared to preoperative baseline recordings in DOPA-OFF (40 ± 10 and 34 ± 12, respectively; [$t(9) = -1.66$; $p = 0.13$], paired t-test), thus making a general aggravation of motor symptoms improbable as a cause for the postoperative theta increase. It is conceivable that the drastic reduction of chronic, longer lasting antiparkinsonian medication following surgery (~40% in this patient sample) may have unmasked some low-frequency components in the spectral distribution, which were less prominent in the pre-operative recordings.

Importantly, compared to pre-operative baseline, STN-DBS also led to a marked reduction of beta- and gamma-power in both absolute and relative resting-state power spectra. There was no longer a statistical difference in absolute beta power between PD patients ON-DBS and controls. Furthermore, ON-DBS was associated with a reduction of beta power compared to OFF-DBS. Thus, STN-DBS had a strong influence on cortical high-frequency activities, particularly in the beta-band. In the context of the TCD framework, pathological elevations of coactivated neighboring thalamo-cortical modules at lower frequencies may result in aberrant high-frequency activity at cortical levels (Llinás et al., 2005; Moazami-Goudarzi et al., 2008). DBS-induced modulation of inhibitory BG output to the thalamus may in turn reduce abnormal thalamo-cortical rhythmicity and normalize high frequency oscillatory power in cortical networks (Llinás et al., 2005).

4.3. Event-related spectral changes

Auditory–motor coordination may depend upon temporally precise neuronal interactions across auditory and motor-related brain areas. A number of recent works have provided evidence for a specific role of beta-band modulation in motor timing (Fujioka et al., 2012; Iversen et al., 2009; Saleh et al., 2010). In PD patients, beta-band activity cannot be modulated as fast and efficiently as in the healthy brain (Doyle et al., 2005; Jenkinson and Brown, 2011). Rhythmic auditory stimuli have recently been demonstrated to result in a periodic modulation of beta activity within the STN (Joundi et al., 2013). At a cortical level, rhythmic auditory stimuli (presented in a passive listening task) also activate motor-related neural networks (Fujioka et al., 2012; Grahn and Brett, 2007; Rao et al., 2001). Fujioka and colleagues observed prominent beta amplitude modulations within supplementary motor area and inferior frontal gyrus during fast auditory pacing (Fujioka et al., 2012). Given the intimate anatomical relationships of these two cortical areas with the STN (Aron and Poldrack, 2006; Haynes and Haber, 2013; Monakow et al., 1978), it is tempting to speculate that STN-DBS may specifically improve cortical beta-band modulation at faster stimulus rates via modulation of centrofrontal cortical activity. This is in fact what we observed in our study.

The beta increase that was found to precede stimulus onset in healthy subjects is consistent with the view of beta-band modulation playing an important role for timing functions. This distinct pre-stimulus component, peaking immediately before the expected stimulus onset, was absent in patients with PD, indicating a timekeeping abnormality for isochronous sounds. Both the analysis of inter-trial coherence and the absence of any correlation between pre- and post-stimulus beta-band ITC values suggest that the broadband response after the stimulus could be related to an auditory evoked response, while the pre-stimulus beta-modulation was not phase-locked to the auditory stimuli, and thus the reported pre-stimulus differences were due to changes in induced beta-band power. This observation is in line with the hypothesis that pre-stimulus beta-band activity could reflect an intrinsically generated neuronal modulation, which may serve predictive functions in rhythm-related tasks (Arnal and Giraud, 2012; Engel and Fries, 2010; Saleh et al., 2010; Teki, 2014).

While pre-stimulus abnormalities were seen for both slow and fast RAS, the post-stimulus beta modulation profile of patients with PD was remarkably unimpaired during slow, but severely impaired during fast RAS, especially when OFF medication. In controls, stimulus-driven beta amplitude modulation was temporally precise, irrespective of pacing frequency, starting only after stimulus presentation. During fast auditory pacing, the timing of this post-stimulus-beta amplitude modulation in patients without dopaminergic therapy became temporally sluggish and was shifted such that it started ramping already before stimulus onset. This may contribute to the loss of temporal alignment with external cues presented at high rates observed in PD patients. Interestingly, an additional evoked component was observed in the theta frequency range, emerging around 0.2 s post stimulus during slow RAS, and 0.1 s at fast RAS. Even if this component was not contained in the time window considered here for the peri-stimulus analysis, is intriguing to consider it as a pre-stimulus phase-reset for the next stimulus as described by Giraud and Poeppel (2012) and Arnal and Giraud (2012).

Before DBS surgery, the stimulus-induced periodic modulations of broadband neural activity displayed excessively large oscillation amplitudes, reminiscent of exaggerated resonance or decreased suppression in response to repeating stimuli (Gulberti et al., 2015). Such abnormal sensory monitoring may hamper the ability of PD patients to respond appropriately to rhythmic auditory input and partially underlie their performance deficits during fast auditory pacing. Transferred into a clinical context, impaired entrainment of fast sensory rhythms could also contribute to the patients' difficulties to synchronize their motor activity with external cues displayed at high rates (Logigian et al., 1991; Yahalom et al., 2004). Furthermore, defective sensory processing may partly underlie dysrhythmic motor deficits of PD patients, such as the so-called "hastening phenomenon". Instead of precisely synchronizing with rhythmic external cues, PD patients involuntarily accelerate their motion. In this condition, impaired sensory processing characterized by abnormally high oscillation amplitudes could trigger activity along motor-related cortex-BG loops, decoupling the patient's motor output from higher order motor control areas and entraining it to a pathological motor rhythm which would then act to involuntarily pace motor actions (Freeman et al., 1993; Logigian et al., 1991; Nagasaki et al., 1978).

Interestingly, a more physiological post-stimulus alignment of beta amplitude modulation was restored by levodopa and STN-DBS — specifically for fast auditory pacing — together with a normalization of the peak size, which was found to be pathologically extended in OFF medication recordings before DBS surgery. The observed tempo-dependence of sensitivity to neuromodulatory treatment suggests a specific role for distinct cortex-basal ganglia circuitries for rhythm-related processing during fast auditory pacing. If sensory entrainment has an influence on auditory–motor coupling, it may thus be proposed that dopamine replacement therapy and STN-DBS may both improve performance of PD patients specifically under conditions of fast auditory pacing.

5. Conclusions

In summary, our results provide evidence for disturbed timekeeping functions directly linked to altered beta-band activity in PD. In particular, we provide evidence for a rate-specific impairment of processing of fast auditory rhythms in PD patients that is both dopamine-dependent and sensitive to therapeutic modulation within cortex-basal ganglia networks. Given the proposed role of beta oscillations for interrelated processes such as rhythm perception, interval timing and sensorimotor coordination, an abnormal reactivity of beta-band responses to auditory stimuli — as in the present study — may contribute to auditory–motor coupling deficits in patients with PD. Conversely, in light of the normalizing effects of levodopa and STN-DBS described here, it is tempting to suggest that both treatments may allow for a more dynamic configuration of sensorimotor networks in response to fast RAS, possibly not only alleviating Parkinsonian impairments of audio–motor synchronization during fast auditory external pacing, but also affecting information processes relying on the extraction of predictable temporal cues in both auditory perception and rhythmic activities (Arnal and Giraud, 2012; Bartolo et al., 2014; Teki, 2014).

Conflicts of interest

Some of the authors (A.G., K.B., W.H., C.B.) have occasionally been reimbursed for travel expenses from Medtronic Inc.

Acknowledgements

We are indebted to all the patients who consented to withdrawal of their medication and deep brain stimulation therapy for the purpose of this study. We are grateful to Kriemhild Saha for help with data recording and to Andrew Sharott for valuable scientific discussions. This work has been funded by the EU (FP7-ICT-270212; A.G., A.K.E.) and the DFG (SFB 936/C8; A.G., C.K.E.M., C.G., A.K.E.).

References

Ahlskog, J.E., Muenter, M.D., Maraganore, D.M., Matsumoto, J.Y., Lieberman, A., Wright, K.F., Wheeler, K., 1994. Fluctuating Parkinson's disease. Treatment with the long-acting dopamine agonist cabergoline. Arch. Neurol. 51, 1236–1241.

Arnal, L.H., Giraud, A.-L., 2012. Cortical oscillations and sensory predictions. Trends in Cognitive Sciences 16 (7), 390–398. http://dx.doi.org/10.1016/j.tics.2012.05.003.

Aron, A.R., Poldrack, R.A., 2006. Cortical and subcortical contributions to stop signal response inhibition: role of the subthalamic nucleus. J. Neurosci. Off. J. Soc. Neurosci. 26, 2424–2433. http://dx.doi.org/10.1523/JNEUROSCI.4682-05.2006.

Bartolo, R., Prado, L., Merchant, H., 2014. Information processing in the primate basal ganglia during sensory-guided and internally driven rhythmic tapping. J. Neurosci. 34 (11), 3910–3923. http://dx.doi.org/10.1523/JNEUROSCI.2679-13.2014.
Bender, R., Lange, S., 2001. Adjusting for multiple testing — when and how? J. Clin. Epidemiol. 54 (4), 343–349. http://dx.doi.org/10.1016/S0895-4356(00)00314-0.
Blin, O., 2003. The pharmacokinetics of pergolide in Parkinson's disease. Curr. Opin. Neurol. 16 (Suppl. 1), S9–S12. http://dx.doi.org/10.1097/00019052-200312001-00003.
Bosboom, J.L.W., Stoffers, D., Stam, C.J., van Dijk, B.W., Verbunt, J., Berendse, H.W., Wolters, E.C., 2006. Resting state oscillatory brain dynamics in Parkinson's disease: an MEG study. Clin. Neurophysiol. 117 (11), 2521–2531. http://dx.doi.org/10.1016/j.clinph.2006.06.720.
Brown, P., 2003. Oscillatory nature of human basal ganglia activity: relationship to the pathophysiology of Parkinson's disease. Mov. Disord. 18 (4), 357–363. http://dx.doi.org/10.1002/mds.10358.
Bruns, A., 2004. Fourier-, Hilbert- and wavelet-based signal analysis: are they really different approaches? J. Neurosci. Methods 137 (2), 321–332. http://dx.doi.org/10.1016/j.jneumeth.2004.03.002.
Carver, F.W., Fuchs, A., Jantzen, K.J., Kelso, J.A.S., 2002. Spatiotemporal analysis of the neuromagnetic response to rhythmic auditory stimulation: rate dependence and transient to steady-state transition. Clin. Neurophysiol. 113 (12), 1921–1931. http://dx.doi.org/10.1016/S1388-2457(02)00299-7.
Cunnington, R., Iansek, R., Bradshaw, J.L., Phillips, J.G., 1995. Movement-related potentials in Parkinson's disease. Presence and predictability of temporal and spatial cues. Brain 118 (4), 935–950. http://dx.doi.org/10.1093/brain/118.4.935.
Delorme, A., Makeig, S., 2004. EEGLAB: an open source toolbox for analysis of single-trial EEG dynamics including independent component analysis. J. Neurosci. Methods 134 (1), 9–21. http://dx.doi.org/10.1016/j.jneumeth.2003.10.009.
Doyle, L.M.F., Kühn, A.A., Hariz, M., Kupsch, A., Schneider, G.-H., Brown, P., 2005. Levodopa-induced modulation of subthalamic beta oscillations during self-paced movements in patients with Parkinson's disease. European Journal of Neuroscience 21 (5), 1403–1412. http://dx.doi.org/10.1111/j.1460-9568.2005.03969.x.
Engel, A.K., Fries, P., 2010. Beta-band oscillations — signalling the status quo? Curr. Opin. Neurobiol. 20 (2), 156–165. http://dx.doi.org/10.1016/j.conb.2010.02.015.
Enzensberger, W., Fischer, P.A., 1996. Metronome in Parkinson's disease. The Lancet 347 (9011), 1337. http://dx.doi.org/10.1016/S0140-6736(96)90987-3.
Eusebio, A., Brown, P., 2009. Synchronisation in the beta frequency-band — the bad boy of parkinsonism or an innocent bystander? Exp. Neurol. 217 (1), 1–3. http://dx.doi.org/10.1016/j.expneurol.2009.02.003.
Fahn, S., Elton, R., UPDRS Program Members, 1987. Unified Parkinson's disease rating scale. In: Fahn, S., Marsden, C., Goldstein, M., Calne, D. (Eds.), Recent Developments in Parkinson's Disease. Macmillan Healthcare Information, Florham Park, NJ, pp. 153–163.
Field, A.P., 2009. Discovering Statistics Using SPSS: (and Sex, Drugs and Rock "n" Roll). Third edition Sage Publications, Los Angeles.
Folstein, M.F., Folstein, S.E., McHugh, P.R., 1975. "Mini-mental state". A practical method for grading the cognitive state of patients for the clinician. J. Psychiatr. Res. 12 (3), 189–198. http://dx.doi.org/10.1016/0022-3956(75)90026-6.
Freeman, J.S., Cody, F.W., Schady, W., 1993. The influence of external timing cues upon the rhythm of voluntary movements in Parkinson's disease. J. Neurol. Neurosurg. Psychiatry 56 (10), 1078–1084. http://dx.doi.org/10.1136/jnnp.56.10.1078.
Freund, H.J., Hefter, H., 1993. The role of basal ganglia in rhythmic movement. Adv. Neurol. 60, 88–92.
Fujioka, T., Trainor, L.J., Large, E.W., Ross, B., 2012. Internalized timing of isochronous sounds is represented in neuromagnetic β oscillations. Journal of Neuroscience 32 (5), 1791–1802. http://dx.doi.org/10.1523/JNEUROSCI.4107-11.2012.
Gasser, T., Bächer, P., Möcks, J., 1982. Transformations towards the normal distribution of broad band spectral parameters of the EEG. Electroencephalogr. Clin. Neurophysiol. 53 (1), 119–124. http://dx.doi.org/10.1016/0013-4694(82)90112-2.
Giraud, A.-L., Poeppel, D., 2012. Cortical oscillations and speech processing: emerging computational principles and operations. Nat. Neurosci. 15 (4), 511–517. http://dx.doi.org/10.1038/nn.3063.
Grahn, J.A., Brett, M., 2007. Rhythm and beat perception in motor areas of the brain. J. Cogn. Neurosci. 19 (5), 893–906. http://dx.doi.org/10.1162/jocn.2007.19.5.893.
Gulberti, A., Hamel, W., Buhmann, C., Boelmans, K., Zittel, S., Gerloff, C., Westphal, M., Engel, A.K., Schneider, T.R., Moll, C.K.E., 2015. Subthalamic deep brain stimulation improves auditory sensory gating deficit in Parkinson's disease. Clin. Neurophysiol. 126 (3), 565–574. http://dx.doi.org/10.1016/j.clinph.2014.06.046.
Hamel, W., Fietzek, U., Morsnowski, A., Schrader, B., Herzog, J., Weinert, D., Pfister, G., Müller, D., Volkmann, J., Deuschl, G., Mehdorn, H.M., 2003. Deep brain stimulation of the subthalamic nucleus in Parkinson's disease: evaluation of active electrode contacts. J. Neurol. Neurosurg. Psychiatry 74 (8), 1036–1046. http://dx.doi.org/10.1136/jnnp.74.8.1036.
Harrington, D.L., Haaland, K.Y., Knight, R.T., 1998. Cortical networks underlying mechanisms of time perception. J. Neurosci. 18, 1085–1095.
Haynes, W.I.A., Haber, S.N., 2013. The organization of prefrontal-subthalamic inputs in primates provides an anatomical substrate for both functional specificity and integration: implications for basal ganglia models and deep brain stimulation. J. Neurosci. 33 (11), 4804–4814. http://dx.doi.org/10.1523/JNEUROSCI.4674-12.2013.
Hebb, A.O., Darvas, F., Miller, K.J., 2012. Transient and state modulation of beta power in human subthalamic nucleus during speech production and finger movement. Neuroscience 202, 218–233. http://dx.doi.org/10.1016/j.neuroscience.2011.11.072.
Herrmann, C.S., Grigutsch, M., Busch, N.A., 2005. 11 EEG Oscillations and Wavelet Analysis. Event-related Potentials: A Methods Handbook 229.
Hoehn, M.M., Yahr, M.D., 1967. Parkinsonism: onset, progression and mortality. Neurology 17 (5), 427–442. http://dx.doi.org/10.1212/WNL.17.5.427.
Hutchison, W.D., Dostrovsky, J.O., Walters, J.R., Courtemanche, R., Boraud, T., Goldberg, J., Brown, P., 2004. Neuronal oscillations in the basal ganglia and movement disorders: evidence from whole animal and human recordings. J. Neurosci. 24, 9240–9243. http://dx.doi.org/10.1523/JNEUROSCI.3366-04.2004.
Huys, R., Studenka, B.E., Rheaume, N.L., Zelaznik, H.N., Jirsa, V.K., 2008. Distinct timing mechanisms produce discrete and continuous movements. PLOS Comput. Biol. 4 (4), e1000061. http://dx.doi.org/10.1371/journal.pcbi.1000061.
Iversen, J.R., Repp, B.H., Patel, A.D., 2009. Top-down control of rhythm perception modulates early auditory responses. Annals of the New York Academy of Sciences 1169 (1), 58–73. http://dx.doi.org/10.1111/j.1749-6632.2009.04579.x.
Jech, R., Mueller, K., Urgošík, D., Sieger, T., Holiga, Š., Růžička, F., Dušek, P., Havránková, P., Vymazal, J., Růžička, E., 2012. The subthalamic microlesion story in Parkinson's disease: electrode insertion-related motor improvement with relative cortico-subcortical hypoactivation in fMRI. PLOS One 7 (11), e49056. http://dx.doi.org/10.1371/journal.pone.0049056.
Jenkinson, N., Brown, P., 2011. New insights into the relationship between dopamine, beta oscillations and motor function. Trends Neurosci. 34 (12), 611–618. http://dx.doi.org/10.1016/j.tins.2011.09.003.
Joundi, R.A., Brittain, J.-S., Green, A.L., Aziz, T.Z., Brown, P., Jenkinson, N., 2013. Persistent suppression of subthalamic beta-band activity during rhythmic finger tapping in Parkinson's disease. Clin. Neurophysiol. 124 (3), 565–573. http://dx.doi.org/10.1016/j.clinph.2012.07.029.
Kühn, A.A., Kupsch, A., Schneider, G.-H., Brown, P., 2006. Reduction in subthalamic 8–35Hz oscillatory activity correlates with clinical improvement in Parkinson's disease. Eur. J. Neurosci 23 (7), 1956–1960. http://dx.doi.org/10.1111/j.1460-9568.2006.04717.x.
Kunesch, E., Binkofski, F., Freund, H.-J., 1989. Invariant temporal characteristics of manipulative hand movements. Exp. Brain Res. 78 (3), 539–546. http://dx.doi.org/10.1007/BF00230241.
Little, S., Pogosyan, A., Kuhn, A.A., Brown, P., 2012. β band stability over time correlates with parkinsonian rigidity and bradykinesia. Exp. Neurol. 236 (2), 383–388. http://dx.doi.org/10.1016/j.expneurol.2012.04.024.
Litvak, V., Jha, A., Eusebio, A., Oostenveld, R., Foltynie, T., Limousin, P., Zrinzo, L., Hariz, M.I., Friston, K., Brown, P., 2011. Resting oscillatory cortico-subthalamic connectivity in patients with Parkinson's disease. Brain 134 (2), 359–374. http://dx.doi.org/10.1093/brain/awq332.
Llinás, R., Urbano, F.J., Leznik, E., Ramírez, R.R., van Marle, H.J.F., 2005. Rhythmic and dysrhythmic thalamocortical dynamics: GABA systems and the edge effect. Trends Neurosci. 28 (6), 325–333. http://dx.doi.org/10.1016/j.tins.2005.04.006.
Logigian, E., Hefter, H., Reiners, K., Freund, H.J., 1991. Does tremor pace repetitive voluntary motor behavior in Parkinson's disease? Ann. Neurol. 30 (2), 172–179. http://dx.doi.org/10.1002/ana.410300208.
Makeig, S., Debener, S., Onton, J., Delorme, A., 2004. Mining event-related brain dynamics. Trends Cogn. Sci. 8 (5), 204–210. http://dx.doi.org/10.1016/j.tics.2004.03.008.
Maris, E., Oostenveld, R., 2007. Nonparametric statistical testing of EEG- and MEG-data. J. Neurosci. Methods 164, 177–190. http://dx.doi.org/10.1016/j.jneumeth.2007.03.024.
Martin, J.P., 1967. The Basal Ganglia and Posture. Pitman Medical, London.
Mattis, S., 1988. Dementia Rating Scale. Psychological Assessment Resources, Inc., Odessa, FL.
McIntosh, G.C., Brown, S.H., Rice, R.R., Thaut, M.H., 1997. Rhythmic auditory–motor facilitation of gait patterns in patients with Parkinson's disease. J. Neurol. Neurosurg. Psychiatry 62 (1), 22–26. http://dx.doi.org/10.1136/jnnp.62.1.22.
Moazami-Goudarzi, M., Sarnthein, J., Michels, L., Moukhtieva, R., Jeanmonod, D., 2008. Enhanced frontal low and high frequency power and synchronization in the resting EEG Of parkinsonian patients. Neuroimage 41 (3), 985–997. http://dx.doi.org/10.1016/j.neuroimage.2008.03.032.
Monakow, K.H., Akert, K., Kunzle, H., 1978. Projections of the precentral motor cortex and other cortical areas of the frontal lobe to the subthalamic nucleus in the monkey. Exp. Brain Res. 33 (3–4), 395–403. http://dx.doi.org/10.1007/BF00235561.
Nagasaki, H., Nakamura, R., Taniguchi, R., 1978. Disturbances of rhythm formation in patients with Parkinson's disease: part II. A forced oscillation model. Percept. Mot. Skills 46 (1), 79–87.
Nakamura, R., Nagasaki, H., Narabayashi, H., 1978. Disturbances of rhythm formation in patients with Parkinson's disease: part I. Characteristics of tapping response to the periodic signals. Percept. Mot. Skills 46 (1), 63–75.
Neufeld, M.Y., Blumen, S., Aitkin, I., Parmet, Y., Korczyn, A.D., 1994. EEG frequency analysis in demented and nondemented parkinsonian patients. Dementia 5 (1), 23–28. http://dx.doi.org/10.1159/000106690.
Neufeld, M.Y., Inzelberg, R., Korczyn, A.D., 1988. EEG in demented and non-demented parkinsonian patients. Acta Neurol. Scand. 78 (1), 1–5. http://dx.doi.org/10.1111/j.1600-0404.1988.tb03609.x.
Olde Dubbelink, K.T.E., Stoffers, D., Deijen, J.B., Twisk, J.W.R., Stam, C.J., Berendse, H.W., 2013. Cognitive decline in Parkinson's disease is associated with slowing of resting-state brain activity: a longitudinal study. Neurobiol. Aging 34 (2), 408–418. http://dx.doi.org/10.1016/j.neurobiolaging.2012.02.029.
Oostenveld, R., Fries, P., Maris, E., Schoffelen, J.-M., 2011. FieldTrip: open source software for advanced analysis of MEG, EEG, and invasive electrophysiological data. Comput. Intell. Neurosci. 2011, 1–9. http://dx.doi.org/10.1155/2011/156869.
Oostenveld, R., Oostendorp, T.F., 2002. Validating the boundary element method for forward and inverse EEG computations in the presence of a hole in the skull. Hum. Brain Mapp. 17 (3), 179–192. http://dx.doi.org/10.1002/hbm.10061.
Perneger, T.V., 1998. What's wrong with Bonferroni adjustments. BMJ 316 (7139), 1236–1238. http://dx.doi.org/10.1136/bmj.316.7139.1236.
Pivik, R.T., Broughton, R.J., Coppola, R., Davidson, R.J., Fox, N., Nuwer, M.R., 1993. Guidelines for the recording and quantitative analysis of electroencephalographic activity in research contexts. Psychophysiology 30 (6), 547–558. http://dx.doi.org/10.1111/j.1469-8986.1993.tb02081.x.

Rao, S.M., Harrington, D.L., Haaland, K.Y., Bobholz, J.A., Cox, R.W., Binder, J.R., 1997. Distributed neural systems underlying the timing of movements. J. Neurosci. 17, 5528–5535.
Rao, S.M., Mayer, A.R., Harrington, D.L., 2001. The evolution of brain activation during temporal processing. Nat. Neurosci. 4 (3), 317–323. http://dx.doi.org/10.1038/85191.
Rothman, K.J., 1990. No adjustments are needed for multiple comparisons. Epidemiology 1 (1), 43–46. http://dx.doi.org/10.1097/00001648-199001000-00010.
Rothman, K.J., 2014. Six persistent research misconceptions. J. Gen. Intern. Med. 29 (7), 1060–1064. http://dx.doi.org/10.1007/s11606-013-2755-z.
Sacks, O., 1999. Awakenings. First edition Vintage Books, New York.
Saleh, M., Reimer, J., Penn, R., Ojakangas, C.L., Hatsopoulos, N.G., 2010. Fast and slow oscillations in human primary motor cortex predict oncoming behaviorally relevant cues. Neuron 65 (4), 461–471. http://dx.doi.org/10.1016/j.neuron.2010.02.001.
Saville, D.J., 1990. Multiple comparison procedures: the practical solution. Am. Stat. 44 (2), 174. http://dx.doi.org/10.2307/2684163.
Savitz, D.A., Olshan, A.F., 1995. Multiple comparisons and related issues in the interpretation of epidemiologic data. Am. J. Epidemiol. 142, 904–908.
Schaal, S., Sternad, D., Osu, R., Kawato, M., 2004. Rhythmic arm movement is not discrete. Nat. Neurosci. 7 (10), 1136–1143. http://dx.doi.org/10.1038/nn1322.
Schneider, T.R., Debener, S., Oostenveld, R., Engel, A.K., 2008. Enhanced EEG gamma-band activity reflects multisensory semantic matching in visual-to-auditory object priming. Neuroimage 42 (3), 1244–1254. http://dx.doi.org/10.1016/j.neuroimage.2008.05.033.
Serizawa, K., Kamei, S., Morita, A., Hara, M., Mizutani, T., Yoshihashi, H., Yamaguchi, M., Takeshita, J., Hirayanagi, K., 2008. Comparison of quantitative EEGs between Parkinson disease and age-adjusted normal controls. J. Clin. Neurophysiol. 25 (6), 361–366. http://dx.doi.org/10.1097/WNP.0b013e31818f50de.
Sharott, A., Gulberti, A., Zittel, S., Tudor Jones, A.A., Fickel, U., Munchau, A., Koppen, J.A., Gerloff, C., Westphal, M., Buhmann, C., Hamel, W., Engel, A.K., Moll, C.K.E., 2014. Activity parameters of subthalamic nucleus neurons selectively predict motor symptom severity in Parkinson's disease. J. Neurosci. 34 (18), 6273–6285. http://dx.doi.org/10.1523/JNEUROSCI.1803-13.2014.
Silberstein, P., 2005. Cortico-cortical coupling in Parkinson's disease and its modulation by therapy. Brain 128 (6), 1277–1291. http://dx.doi.org/10.1093/brain/awh480.
Sinanović, O., Kapidzić, A., Kovacević, L., Hudić, J., Smajlović, D., 2005. EEG frequency and cognitive dysfunction in patients with Parkinson's disease. Med. Arh. 59, 286–287.
Singh, A., Plate, A., Kammermeier, S., Mehrkens, J.H., Ilmberger, J., Bötzel, K., 2013. Freezing of gait-related oscillatory activity in the human subthalamic nucleus. Basal Ganglia 3 (1), 25–32. http://dx.doi.org/10.1016/j.baga.2012.10.002.
Soikkeli, R., Partanen, J., Soininen, H., Pääkkönen, A., Riekkinen Sr, P., 1991. Slowing of EEG In Parkinson's disease. Electroencephalogr. Clin. Neurophysiol. 79 (3), 159–165. http://dx.doi.org/10.1016/0013-4694(91)90134-P.
Stoffers, D., Bosboom, J.L.W., Deijen, J.B., Wolters, E.C., Berendse, H.W., Stam, C.J., 2007. Slowing of oscillatory brain activity is a stable characteristic of Parkinson's disease without dementia. Brain 130 (7), 1847–1860. http://dx.doi.org/10.1093/brain/awm034.
Szirmai, I., 2010. How does the brain create rhythms? Ideggyogy. Sz. 63, 13–23.
Tallon-Baudry, C., Bertrand, O., Delpuech, C., Pernier, J., 1996. Stimulus specificity of phase-locked and non-phase-locked 40 Hz visual responses in human. J. Neurosci. 16, 4240–4249.
Tanaka, H., Koenig, T., Pascual-Marqui, R.D., Hirata, K., Kochi, K., Lehmann, D., 2000. Event-related potential and EEG measures in Parkinson's disease without and with dementia. Dement. Geriatr. Cogn. Disord. 11 (1), 39–45. http://dx.doi.org/10.1159/000017212.
Teki, S., 2014. Beta drives brain beats. Front. Syst. Neurosci. 8, 155. http://dx.doi.org/10.3389/fnsys.2014.00155.
Temperli, P., Ghika, J., Villemure, J.-G., Burkhard, P.R., Bogousslavsky, J., Vingerhoets, F.J.G., 2003. How do parkinsonian signs return after discontinuation of subthalamic DBS? Neurol. 60 (1), 78–81. http://dx.doi.org/10.1212/WNL.60.1.78.
Toma, K., Mima, T., Matsuoka, T., Gerloff, C., Ohnishi, T., Koshy, B., Andres, F., Hallett, M., 2002. Movement rate effect on activation and functional coupling of motor cortical areas. J. Neurophysiol. 88, 3377–3385. http://dx.doi.org/10.1152/jn.00281.2002.
Tomlinson, C.L., Stowe, R., Patel, S., Rick, C., Gray, R., Clarke, C.E., 2010. Systematic review of levodopa dose equivalency reporting in Parkinson's disease. Mov. Disord. 25 (15), 2649–2653. http://dx.doi.org/10.1002/mds.23429.
Yahalom, G., Simon, E.S., Thorne, R., Peretz, C., Giladi, N., 2004. Hand rhythmic tapping and timing in Parkinson's disease. Parkinsonism Relat. Disord. 10 (3), 143–148. http://dx.doi.org/10.1016/j.parkreldis.2003.10.001.